Fall 2014

In vitro evaluation of carbon-nanotube-reinforced bioprintable vascular conduits

Farzaneh Dolati
University of Iowa

IN VITRO EVALUATION OF CARBON-NANOTUBE-REINFORCED BIOPRINTABLE VASCULAR CONDUITS

by

Farzaneh Dolati

A thesis submitted in partial fulfillment
of the requirements for the
Master of Science degree in Industrial Engineering
in the Graduate College of
The University of Iowa

December 2014

Thesis Supervisor: Assistant Professor Ibrahim Tarik Ozbolat

Graduate College
The University of Iowa
Iowa City, Iowa

CERTIFICATE OF APPROVAL

_____

MASTER'S THESIS

_____

This is to certify that the Master's thesis of

Farzaneh Dolati

has been approved by the Examining Committee
for the thesis requirement for the Master of Science
degree in Industrial Engineering at the December 2014 graduation.

Thesis Committee: _____
Ibrahim T. Ozbolat, Thesis Supervisor

_____
David M Cwiertny

_____
Shaoping Xiao

To my husband, Alireza Mofidi and my parents for their love, support and encouragement.

ACKNOWLEDGEMENTS

Completing my MS. degree is one the most challenging adventures of my life which was not possible without the support of many people.

I would like to express my sincere gratitude to my supervisor, Dr. Ibrahim Tarik Ozbolat. Your dedication to invaluable instructions and many thoughtful suggestions ever cannot be overstated.

I would like to express my deep gratitude and respect to my committee members, Dr. David M Cwiertny and Dr. Shaoping Xiao, whose advice and insight were invaluable to me. I would also like to thank Yin Yu for cell viability and tissue histology tests, and Yahui Zhang for degradation and swelling test. My research would not have been possible without their help. Many thanks to Dr. Edward Sander and his student Aribet M De Jesus for providing the mechanical testing unit, Biotense Perfusion Bioreactor (ADMET, Inc. Norwood, MA).

Thanks are given to all my friends and colleagues, who are too many to name here, but have given me consistent help and support. Our academic discussions helped us to obtain fruitful results and always brought ideas to me during my research.

A special thanks to my husband and my parents. Words cannot express how grateful I am to my family; for all of the sacrifices that you have made on my behalf. Thanks for teaching me about hard work and self-respect, about persistence and about how to be independent. I hope this work makes you proud.

ABSTRACT

Vascularization of thick engineered tissue and organ constructs like the heart, liver, pancreas or kidney remains a major challenge in tissue engineering. Vascularization is needed to supply oxygen and nutrients and remove waste in living tissues and organs through a network that should possess high perfusion ability and significant mechanical strength and elasticity. In this thesis, we introduce a fabrication process to print vascular conduits directly, where conduits were reinforced with carbon nanotubes (CNTs) to enhance their mechanical properties and bioprintability. The generation of vascular conduit with a natural polymer hydrogel such as alginate needs to have improved mechanical properties in order to biomimic the natural vascular system. Carbon nanotube (CNT) is one of the best candidates for this goal because it is known as the strongest material and possesses a simple structure.

In this thesis, multi-wall carbon nanotube (MWCNT) is dispersed homogenously in the hydrogel and fabricated through an extrusion-based system.In vitro evaluation of printed conduits encapsulated in human coronary artery smooth muscle cells was performed to characterize the effects of CNT reinforcement on the mechanical, perfusion and biological performance of the conduits. Perfusion and permeability, cell viability, extracellular matrix formation and tissue histology were assessed and discussed, and it was concluded that CNT-reinforced vascular conduits provided a foundation for mechanically appealing constructs where CNTs could be replaced with natural protein nanofibers for further integration of these conduits in large-scale tissue fabrication. It was concluded that MWCNT has a significant effect on mechanical properties, vascular conduit swelling ratio and biological characterization in short-term and long-term cellular viability.

PUBLIC ABSTRACT

Tissue engineering is an existing area which offering the potential for regenerating almost every tissue and organ of the human body particularly to address the tremendous shortage of donor tissues for transplantation procedures. Tissue engineers Integrates a variety of engineering principals and biological science discipline to develop biological substitutes that can be used to replace diseased/ damaged tissues.

Cardiovascular diseases have remained one of the leading causes of death during the past decade, one in every five American die due to Coronary Heart disease, however fewer progress have been made in engineering small diameter vascular grafts. In addition, Shortage numbers of donors for tissue replacement (18 people die each day waiting for an organ) and risk of organ transplantation for patient are the main reasons to perform this study.

In this research, vascular conduits were fabricated through an extrusion based bioprinting system. The generation of vascular conduits with natural polymer such as alginate needs to have improved mechanical properties in order to biomimic the natural blood vessel. Carbon nanotube (CNT) is one of the best candidates for this goal because it is known as the strongest material and possesses a simple structure. In this work, multi-wall carbon nanotubes (MWCNT) were dispersed homogenously in alginate and printed using an extrusion-based system. The effects of using MWCNT as a reinforcement agent were investigated in mechanical, swelling and degradation tests. Cell viability studies were conducted to explore effects of MWCNT on short term biocompatibility as well as long-term tissue formation.

TABLE OF CONTENTS

LIST OF FIGURES

CHAPTER I

INTRODUCTION

Cardiovascular diseases have remained one of the leading causes of death during the past decade. The U.S. Department of Health and Human Services (DHH) reported that around 79 people receive organ transplants every day and, due to a shortage of donors, every year around 18 people die in the process of finding a donor [1]. Another challenge for patients who have found donors is to determine whether or not their serotypes match the donors' serotypes. In addition, there is a lifelong fear of transplant rejection when a patient receives an organ or tissue from other donors. Because there are not enough donors for tissue replacement and because of other difficulties in the transplant process, there is a need to regenerate organs and tissues with vascular conduits.

Tissue engineering is a field that combines the principles of engineering with the biological sciences to generate a functional living tissue structures with the potential for growth to replace or reconstruct diseased tissue. The goal of tissue engineering research is the development of reconstituted living cells and other natural substances in the form of biological substitutes that can be used to repair, maintain or enhance tissue functions. In tissue engineering, relevant cells grow in vivo and in vitro into required 3D organs or tissues. The promising advance in this field is that, in addition to reducing the wait time for finding a donor, it is possible to get the cells from the patient's own body to regenerate the malfunctioning tissue, eliminating worries about rejection and immune response in the future. Since the 1970s, when tissue engineering was introduced, researchers have been interested in fabricating several noncomplex human organs such as skin [2-5], vascular

graft [6-11], bone [12, 13] and cartilage [14, 15]. Nowadays researchers focus on more complex human organs like liver [16, 17], heart [18, 19] and kidney [20, 21].

Generating noncomplex organs like skin is more achievable since they have simple geometry, low cell oxygen consuming rates and fewer requirements for blood vessels. Vascularization of thick engineered tissue structures like the heart, liver and kidney remains a major challenge in tissue engineering. Vascularization is needed to supply oxygen and nutrients and remove waste in the live tissue. The artificial vascular conduit biomimics the natural vascular system with three distinct tissue layers composed of different cells that exhibit different functions, such as providing oxygen and nutrients to cells as well as taking away the waste [22-24].

Vascular tissue engineering fabrication could be divided in two major strategies type: scaffold-based tissue engineered vascular conduits or cell-based tissue engineered vascular conduits [25]. Scaffold is a temporary substrate for cells to growth and proliferate. Cells will be seeded on the scaffold and cultured in the bioreactor in order to regulate cell differentiation until the live cells grow and distribute uniformly in the scaffold. In order to enhance cell attachment, cell adhesion molecules for instance laminin (LN) and cadherin could be used to coat the scaffold when the scaffold is designed [26].

Several techniques have been developed to fabricate scaffolds such as solvent-casting particulate-leaching[27, 28], fibers bonding [29] gas foaming [30], freeze drying [31, 32], spinning [33]. The major limitations for scaffold based fabrication tissue engineering are the difficulty in controlling spatial distribution of pores and construction of internal channels, biocompatibility, mechanical properties and easy manipulation [34].

In addition there are limited clinical application in human body and needs more reassessment and modification.

Due to the limitation of scaffold-based tissue engineering and failure of cell to cell interaction the Scaffold free based or cell-based tissue engineering technique has been introduced. In This method cells are capable to manufacture their own extracellular matrix (ECM). There are several techniques to fabricate a vascular conduit by means of this method such as, decellurization [35, 36], cell sheet engineering [8, 37], biodegradable synthetic polymer-based constructs [38, 39] and natural biomaterial-based blood vessel grafts [8, 40, 41], bio printing [8], cell printing [42]. In tissue decellurization method, which is totally composed of extracellular matrix (ECM) and has high mechanical properties and more importantly high biocompatibility in comparison with other methods [43-46]. The extracellular matrix is a component surrounded the cells and provides structure and biochemical support. The disadvantage of this method is shrinkage during the decellularization process. The next method is the cell sheets method, which has a unique mechanical property of an artery due to having the best burst pressure results [38].The third method uses biodegradable synthetic polymer-based constructs, which may have toxic or acidic byproducts during the biodegradation process, may affect the cell culture environment, or may have some difficulties in cell attachment and signaling due to lack of reactive groups on the surface chemistry [8, 39]. The last method uses natural biomaterial-based blood vessel grafts and has the best biocompatibility and degradability for cell attachments and proliferation. The main problem with this method is the low mechanical properties of natural polymers [40, 41, 47].

Among all these techniques, bio printing is a novel technique in fabrication 3D tissue construct. In this technique, cells are seeded while fabrication process of 3D tissue is occurred simultaneously, cells are printed layer by layer through a computer-controlled robotic 3D printer [34].since this technique provides precision 3D positioning of different type of cells with high density of cells [48], it is a solution for the major challenge in tissue engineering field which is fabricating vascular system in thick organ tissue.

Artificial blood vessels save the lives of many patients, especially in bypass applications such as shunts for dialysis or treatment of blood vessel failure; they also can be used as supplement vessels for the fabrication of engineered thick tissues [37]. Based on the application of artificial vascular tissues, several features are required, including perfusability, mechanical elasticity and strength for pulsatile stress and suture retention, diffusion properties, and the capability to transport nutrients, oxygen and waste [23, 49]. In order to develop vascular constructs biomimetically, one should thus consider incorporating these requirements during the fabrication process by choosing proper biomaterials and fabrication methods [23, 50]. Newly developed biomaterials or novel modifications of existing biomaterials have great potential in the development of clinically important tissue engineering applications. Chemical composition, mechanics of breakdown, degradation products, mechanical properties, cell-surface interactions and clinical limitations are all influential in biomaterial development [25, 51-53].

Biomaterials which are used in vascular tissue engineering are classified into two groups:

1. Synthetic polymers: The major class of synthetic polymers, which are biodegradable and widely usable in tissue fabrication, includes poly lactic acid (PLA), poly glycolic acid (PGA) and their copolymers poly lactic acid co glycolic Acid (PLGA) and polycaprolactone (PCL). Although these synthetic polymers are biocompatible, they are not popular due to their toxicity; an acidity byproduct during the biodegradation process could damage the cell culture processes [26, 54, 55].
2. Natural polymers (Biopolymers): Natural hydrogels have great biocompatibility and degradability and also provide a suitable environment for cell culture, attachment and proliferation. Natural polymers, such as protein or carbohydrate polymers (collagen, gelatin, alginate and chitosan), have better biocompatibility than synthetic polymer gels. However, they have limitations in mechanical properties (physical parameters), which are very important design criteria in tissue engineering [56]. Therefore, modifying their properties by means of adding other polymers or fibers can be helpful.

There are several criteria for selecting the proper biomaterial for tissue engineering, such as manufacturing feasibility, sufficient commercial availability, capability to form into the final design, mechanical properties that adequately address short-term function and do not interfere with long-term function, low or negligible toxicity of degradation products, drug delivery compatibility and physical parameters in order to control the structure and function of the tissue, biological properties to be able to promote cellular interaction and regulate cellular functions and biocompatibility to provide proper environment for cell to grow and proliferation [23, 56, 57].

Hydrogels are among the most commonly employed matrices in tissue engineering because they are biocompatible, are able to facilitate nutrient/oxygen transport, and are highly hydrated three-dimensional (3D) networks that structurally resemble the extracellular matrix (ECM) [23, 50, 57]. The criteria for selecting proper material for tissue engineering are directly based on their material chemistry, molecular weight, solubility, shape and structure, surface energy, water absorption degradation and erosion mechanism [51-53].

One of the most common natural hydrogels is alginate, which is derived from brown seaweed and can be synthesized by bacteria[58]. Alginate is appropriate for fabricating a tissue construct because it is a natural polymer, is abundant in nature, is highly biocompatible, and has low toxicity and macromolecular properties similar to those of natural ECM [58]. It also crosslinks at room temperature, without pH changes and in an environment where no external toxic material can denature drugs or damage or kill living cells. Gelation occurs through a crosslinking mechanism in which divalent cations ionically interact with carboxylate anions of G units, forming ionic bridges between different polymer chains. Alginates are highly absorbent (up to 15-20 times their own weight) and non-adherent. The main advantage of the gelation process is that it occurs gently under mild conditions and at room temperature without producing any toxic components. Alginate could be applied in several areas. It used as synthetic extracellular matrices (ECMs) for cell immobilization, cell transplantation and tissue engineering due to its physical properties that are similar to natural tissues [51, 58]. Due to the lack of hydrophobic interactions, alginate hydrogel gives an advantage of encapsulation all drugs and even DNA without causing damage. When biomaterial solution and crosslinker

solution are fed into coaxial nozzle simultaneously, sodium alginate through the feed tube section and the crosslinker through the inner section as presented in figure 3.3, the gelation of alginate vascular conduits occurs immediately, providing tubular conduits [59].

The process of coaxial printing allows printing vascular conduits in any desired shape in 3D [60]. More detailed information about the process of coaxial printing and coaxial nozzle is presented in Section 3.3.

In this thesis, the goal is to modify alginate properties by adding carbon nanotubes to prepare composite solutions for fabricating vascular conduits. The composite solution consists of a biocompatible polymer as a matrix and is reinforced with fibers. Determining the orientation, de-aggregation and dispersion of reinforcement by fibers can increase the strength and resistance to deformation of the composite vasculature [49, 56, 58]. By homogeneously dispersing reinforced fibers, the interfacial interaction with the matrix can increase, resulting in the enhancement of the mechanical properties of the composite [49, 58, 60, 61]. In summary, multi wall carbon nano-tube (MWCNT) reinforced alginate vascular conduits were printed using a coaxial bioprinting process [62]. Mechanical properties were evaluated and compared with vascular conduits made of plain alginate with different concentrations of alginate and dosages of MWCNTs. In addition, the elongation and diffusion rate of the vascular conduit were investigated. Furthermore, cell viability tests and tissue histology studies were conducted to evaluate the effects of MWCNTs on cell viability, matrix deposition and the tissue generation process.

The content of this thesis is structured as below:

Chapter 2: Literature review

Chapter 3: Materials and methods

CHAPTER II

LITERATURE REVIEW

To date, the standard treatment for blood vessels damages is still autologous blood vessels transplantation which is depended on patient's condition to have a suitable autologous tissue and restore it with damage one to serve as a vascular conduits [63]. The main drawbacks for this treatment are, occluded vessels or the risk of infection, cancer or cardiovascular diseases[48, 63]. In order to overcome these drawbacks, fabricating artificial vascular conduits are required. Fabricating a vascular system in artificial organ tissue is one of the major challenges and an important area of research in the tissue engineering field. An artificial vascular system needs to mimic the natural one in the human body and, more importantly, it needs to be capable of transporting nutrients, oxygen and waste. Hence, vascularization of a thick engineered tissue structure remains a major challenge in tissue engineering. Fabricating a vascular system with the capability of providing oxygen and nutrients to the cells in engineered tissue would represent great progress in the tissue engineering field [22, 24, 64].

Since the cells are so sensitive to the environment and it is very important to have higher cell viability, In order to promote this factor, several factors should be considered such as material properties, surface treatment, substrate mechanics and scaffold degradation kinetics[8, 23, 25]. Natural biomaterials are widely used in tissue engineering due to their biocompatibility and biodegradability; however, their mechanical properties need to be enhanced. Several researchers have come up with different methodologies for improving the mechanical properties of the natural biomaterials [61, 65-67].

One approach to improving the mechanical properties of alginate is the integration of carbon nanotubes (CNTs), which are among the strongest materials known and possess a simple structure [65, 68, 69]. In particular, single-walled carbon nanotubes (SWCNTs) and MWCNT have unique mechanical strength and stiffness, have a high aspect ratio, are lightweight, and are flexible and low density [65]. Therefore, CNTs have outstanding potential as reinforcements in composite materials. Several researchers have used CNTs in their studies to enhance mechanical properties and have evaluated cell viability and proliferation in tissue scaffolds [61, 70, 71].

Based on the results of those researchers, CNTs are a suitable material for enhancing mechanical properties and an acceptable substrate for cells to grow on [56, 70, 72, 73]. Mattson et al. [73] successfully used CNTs as suitable substrates for nerve cell growth. In that study, the flat substrate of MWCNTs was coated with a 4-hydroxynonenal bioactive molecule to create multiple neuritis. Then neurons were grown on that substrate and generated a number of branches. However, neurons that were grown on the substrates without CNTs could generate only a few branches since they did not resemble the cellular surfaces and ECM in the body. Hu et al. [72] used the same method as Mattson et al. [73] to incorporate CNTs as a substructure in order to culture the hippocampal neuronal growth. The coated surface with MWCNTs was able to control the neuritis outgrowth, generate longer neuritis length and control the branching pattern. Mazzatena et al. [71] proved that tissue-specific development of seeded cells could be enhanced by CNTs. They grow hippocampal cells on the single wall carbon nan-tube (SWCNT) substrate and used high electrical conductivity properties of carbon nano-tube to increase neuronal responses similar to brain circuit activity.

In addition, the study by Lobo et al. [70] showed that it was possible to achieve higher cell viability and cell adhesion on MWCNT dense films. fibroblast L929 mouse cells were used and after the cells growth and proliferate on the vertical aligned carbon nano-tube film, 100% cell viability achieved in 96 hours on incubation. The first layer on the CNT surface was spread by fibroblast cells which block the interaction of the rest of cells with the nanotube, hence, it increase the adhesion level of cells. Yildirim et al. [68] investigated whether SWCNT-incorporated scaffolds had better cell attachment and proliferation, thus having more viable cells after seven days in comparison with non-reinforced scaffold. Tissue scaffolds were fabricated by means of a freeform fabrication technique through layer-by-layer deposition of material. The mechanical test showed that the composite reinforced with 1% SWCNT had higher tensile strength since the structure of the scaffold has higher mechanical strength. Verdejo et al. [74] showed the increase of osteoblastic cell proliferation and differentiation by adding CNTs. MWCNT was loaded and distributed in the 3D poly urethane (PU) foams as a reactive poly urethane carbon nanotube foams, CNTs were very active on the pore surfaces of the scaffold and the cell studies of Osteoblastic cells (bone cells) proliferation and differentiation showed that CNT toxicity doesn't affect on the cells viability as well as proliferation and differentiation.

.

CHAPTER III

MATERIALS AND METHODS

Tissue engineering is an existing area that offers the potential to regenerate almost every tissue and organ in the human body, and is particularly aimed at addressing the tremendous shortage of donor tissues for transplantation procedures. The artificial vascular conduit biomimics the natural vascular system with three distinct tissue layers composed of different cells that exhibit different functions, such as providing oxygen and nutrients to cells and taking away the waste [22-24]. Several tissue engineering strategies have addressed suitable materials that could mimic the native vascular tissue's mechanical properties and also promote cell growth and cell viability and facilitate extracellular matrix (ECM) production [25, 43, 75]. Materials for vascular replacement should be biomimetic in a way that the capacity to mimic the natural ECM is improved in order to regulate the extent and strength of cell adhesion, growth activity and cell differentiation to the desired vascular tissue [25, 43, 75]. This chapter investigates the materials and methods to fabricate vascular conduits as well as improve mechanical properties.

3.1 Materials

Sodium alginate (purchased from Sigma Aldrich, United Kingdom) and calcium chloride ($CaCl_2$) (purchased from Sigma Aldrich, Japan) were used to fabricate vascular conduits. Solutions of 3–4% (w/v) sodium alginate were dissolved in deionized water and placed in a shaker for 10 h at 120 rpm. Similarly, 4% (w/v) $CaCl_2$ solutions was prepared using deionized water [60]. These concentrations were preferred due to the manufacturability of functional conduits based on our earlier experiments.

Pristine MWCNTs were purchased from Nano Labs Inc., USA. For preparation of the CNT solution, a functionalization method and an acid-washing treatment of nitric acid 70% (HNO3) were used to oxidize the pristine CNTs [76]. Carbon nanotubes (100 mg) were dispersed by sonication in 250 ml for 1 h. Then, the mixture of MWCNT HNO_3 was refluxed at 140 ˚C for 1.5 h while stirring. Next, the mixture was cooled down to room temperature. The concentration of the suspension was 70% (w/v). For the first four composite samples, 1% (w/v) and 0.5% (w/v) MWCNT were dissolved in alginate solutions with 3% and 4% concentrations, and each sample was placed on a stirrer for one day until the CNTs were dissolved homogeneously. Two samples of alginate only with concentrations of 3% and 4% (w/v) were also produced.

3.2 Cell preparation

Human coronary artery smooth muscle cells (HCASMCs) (Life Technologies, MA, USA) were used in this study to test cell viability when encapsulated in CNT-reinforced vascular conduits. The HCASMCs were cultured at 37 ºC in 5% CO_2 in smooth muscle cell growth media (Life Technologies, MA, USA) supplemented with smooth muscle cell growth supplement (Life Technologies, MA, USA), 100 µg μl^{-1} penicillin, 100 µg ml^{-1} streptomycin and 2:5 µg μl^{-1} Fungizone. The culture media was changed every other day. Cells were harvested until we achieved a sufficient amount for bioprinting. After harvesting, cells were centrifuged down, resuspended in a 4% sodium alginate and 1% MWCNT solution, and gently mixed by a vortex mixer to get uniform distribution. The cell seeding density used in this study was 10×10^6 cells ml^{-1}.

3.3 Fabrication of carbon-nanotube-reinforced vascular conduits

The experimental setup (Figures 3.1 (a) and (b)) consisted of a single-arm robotic printer (EFD Nordson, East Providence, RI) with a motion unit, a coaxial nozzle (Figures 3.1 (a) and 3.2 (a)), a syringe pump (New Era Pump System Inc., Farmingdale, RI) and a pressure regulator (EFD Nordson, East Providence, RI) for composite solutionand $CaCl_2$ solution as the crosslinker.

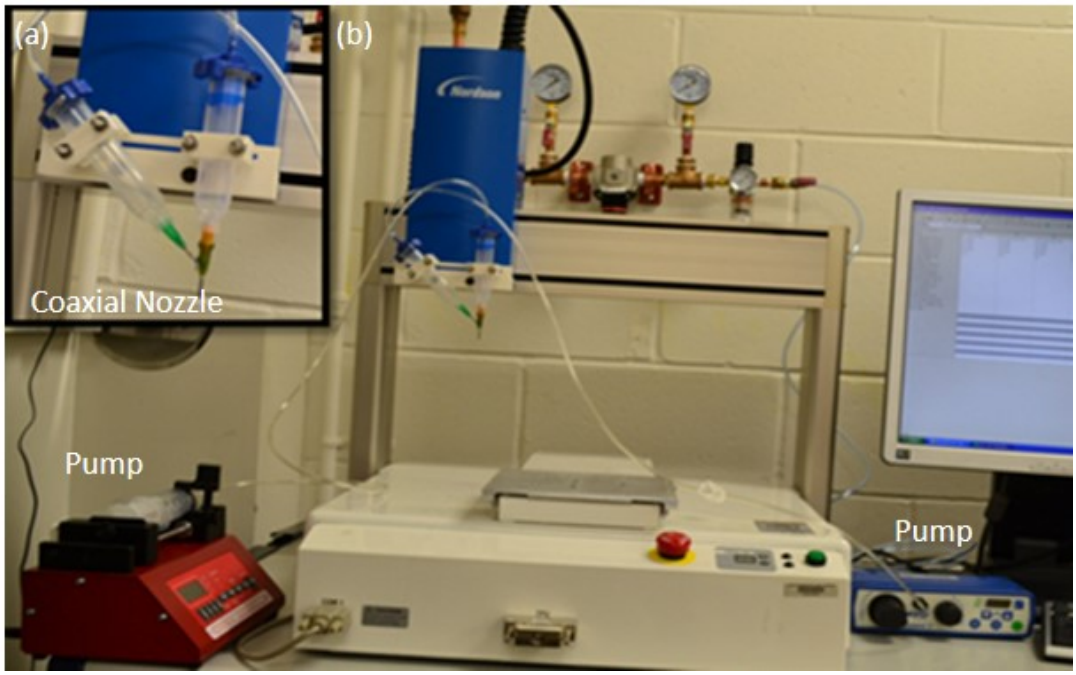

Figure 3.1

The experimental setup for fabricating vascular conduits: (a) the coaxial nozzle system, (b) the bioprinter platform

The coaxial nozzle was mounted on the bioprinter unit. The coaxial nozzle had three sections: a feed tube, an outer tube and an inner tube (Figure 3.2 (a)). The composite solution was fed from the feed tube, and the inner tube was used to feed the crosslinker solution. The composite solution flowed into the space between the inner and outer tubes (Figure 3.2 (a)). A dispenser was connected to the syringe barrel, which contained the composite solution, and the syringe pump was connected to the barrel with the $CaCl_2$ solution (Figure 3.2 (b)).

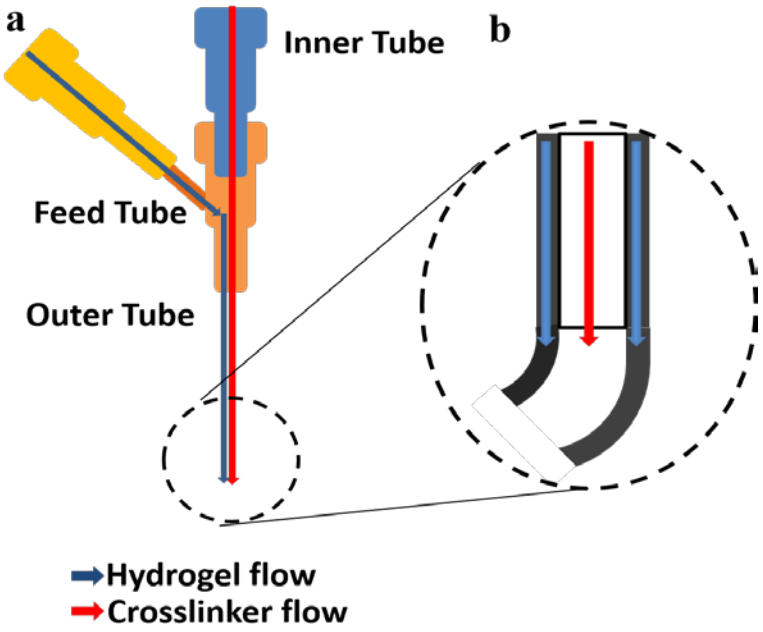

Figure 3.2

The coaxial nozzle section: (a) cross sectional view of coaxial nozzle, (b) zoom-in view of extrusion process

3.3.1 Fabrication process

The sodium alginate was dispensed from the sheath section of the nozzle, while the crosslink solution was dispensed from the core section by compressed air. When the two solutions contacted, the vascular conduits were formed and printed. The coaxial assembly used in this study had a 25 gauge (260 μm inner diameter (I.D.), 510 μm outer diameter (O.D.)) inner needle and a 14 gauge (1600 μm I.D., 2110 μm O.D.) outer needle. The dispensing rate for the $CaCl_2$ solution was 16 ml min^{-1} and 12 ml min^{-1} for 4% and 3% plain alginate, respectively. The dispensing pressure for composite solution was 20.7 kPa and 13.8 kPa for 4% and 3% alginate, respectively.

3.4 Mechanical testing

3.4.1 Tensile test

All printed vascular conduits were soaked in the $CaCl_2$ solution for 24 h in order to minimize the effect of residence time in the $CaCl_2$ solution. Three different random segments for each sample were fabricated to evaluate mechanical characterization using a Biotense Perfusion Bioreactor (ADMET, Inc. Norwood, MA). The mechanical testing unit consisted of a linear actuator, sample grips, a bioreactor frame and a 250 g load cell. The load cell and closed-loop servo-controlled actuator can measure a maximum tensile load of 2 N and provide a stroke of 25 mm, respectively. Load-displacement data was recorded at 1 Hz through a data acquisition system (MTest Quattro System, ADMET, Inc.

The samples were mounted in the grips between pieces of sandpaper (to minimize slip), leaving a sample gauge length of 6-8 mm for mechanical loading. The vascular

conduits were loaded to failure at a rate of 10 mm min $^{-1}$. Samples that failed at the edge of grips were discarded from analysis.

By having the displacement and load information data which were recorded through the data acquisition system tensile strength was founded through $\sigma = L/A$ where σ represents the stress, L represents the tensile load on the Biotense Perfusion Bioreactor (ADMET, Inc. Norwood, MA) and A represents the area of the vascular conduit samples under tensile. In order to calculating the area of the vascular conduits since it was in hollow channel shape, the coaxial nozzle inner and outer needle gauge size were used. For calculating Elastic Modulus, first dimension of each vascular conduit samples were measured before and after the experiment and then strain was founded through $\varepsilon = \Delta L/L$, where ε represents strain , ΔL represents the change in length of the samples and L represents the original length of vascular conduit sample. Finally elastic modulus (E) were found out through Hooke's Law $E = \sigma/\varepsilon$. The ultimate strain is founded through the maximum strain that a vascular conduit sample can be failed.

3.5 Burst pressure

The estimated burst pressure (*BP*) was calculated from ultimate tensile strength (*UTS*) measurements by rearranging the Laplace law for a pressurized thin-walled hollow cylinder [16], where *BP* is the estimated burst pressure (mmHg), *T* represents the wall thickness (μm) of conduits, and *LD* represents the unpressurized lumen diameter (μm) [59, 67]

$$BP = 2\frac{UTS \times T}{LD} \tag{1}$$

3.6 Perfusion test

The main function of vascular conduits is to provide nutrients and oxygen to surrounding tissues as well as take away the waste. In order to develop vascular conduits biomimetically, it is essential to evaluate the permeability capability of the engineered vascular conduits. Thus, a perfusion system, which consisted of a media reservoir, a peristaltic pump (ISMATEC, IDEX Corporation, Glattbrugg Switzerland) and a perfusion chamber (with a cover to prevent evaporation) (see Figure 3.4 (a)), was developed. A peristaltic pump was selected to provide pulsatile media flow, and cell media was perfused from the media reservoir, through the pump and the vascular conduit, and pumped back to the media reservoir. Gauge 25 (0.25 mm I.D., 0.52 mm O.D.) needles were inserted into the fabricated vascular conduits. Surgery clips were used to fix the vascular conduits during perfusion without leakage. Several combinations of fabrication parameters (i.e., composite dispensing pressure and $CaCI_2$ dispensing rate) were tested to obtain the ideal core diameter to obtain a best match for a gauge 25 needle. The criteria for the fabrication parameter selection was that the lumen diameter of the dispensed vascular conduit should be exactly same as the size of a 25 gauge needle's outer diameter, such that the needle could be inserted into the vascular conduit tightly and no leakage should be allowed at the connection of the conduit and the needle.

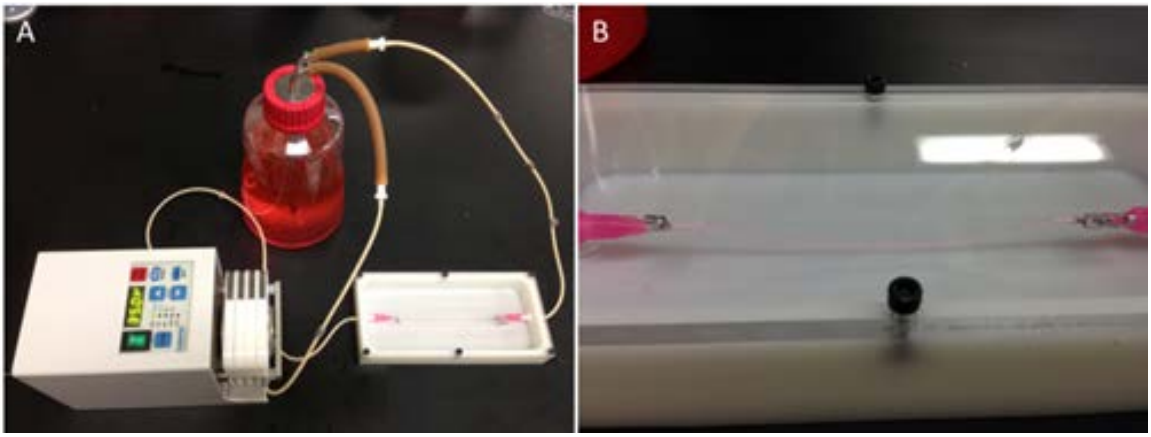

Figure 3.3

Experimental setup for perfusion test: (A) perfusion system consists of three parts, a cell media reservoir, a pump and a perfusion chamber, and (B) perfusion chamber has a clear cover to prevent evaporation.

The original length of the perfusable vascular conduits was fixed at 8 cm. Perfusion experiments were conducted with a 20 ml min $^{-1}$ perfusion flow rate for 1 h. Elongation and diffusion rate measurements were conducted immediately after 1 h of perfusion. The diffusion rate and elongation were measured for 4% alginate vascular conduits, 4% alginate 0.5% MWCNT-reinforced vascular conduits, and 4% alginate 1% MWCNT vascular conduits.

3.7 Dehydration and swelling studies

All printed vascular conduits were soaked in 4% $CaCl_2$ for 30 minutes, hence all the conduits were fully cross-linked. For the swelling and degradation studies, we first needed to dehydrate the vascular conduits by having them at room temperature for 4 days.

Then the dehydrated vascular conduits were soaked in the phosphate buffer saline (PBS). The swelling ratio (*SR*) was calculated using the following equation:

$$SR = \frac{W_i - W_d}{W_d} \times 100\% \quad (2)$$

Where W_i is the instant alginate vascular conduit weight at the measurement moments, W_d is the dehydrated alginate vascular conduit weight.

3.8 Cell viability

Immediately after printing, samples were washed with Hank's balanced salt solution (HBSS) supplemented with 100 U ml^{-1} penicillin, 100 μg ml^{-1} streptomycin and 2.5 μg ml^{-1} fungi zone for sterilization before incubation. After washing, vascular conduits were cultured at 37 ºC in 5% CO_2. Cell viability assays were performed immediately after printing, as well as after three days in vitro culture to evaluate cell survival. Plain vascular conduits with alginate served as a control group. Vascular conduits 5 cm in length were printed for each sample. For cell viability analysis, samples underwent fluorescent microscopic examination. Vascular conduits were stained with calcium acetoxy methyl ester (calcein AM) and ethidium homodimer2 (Invitrogen™ Life Technologies, U.S.A.) at a concentration of 1.0 mM each. Calcein AM stains live cells green, while ethidium homodimer2 stains dead cells red. After a 30 min incubation period, vascular conduits were imaged under a Leica fluorescent microscope (Leica Microsystems Inc., Buffalo Grove, IL, USA). Images were collected from three different locations randomly chosen from each

sample. Image J (National Institutes of Health, Bethesda, MD, USA) was used for automated counting of red- and green-stained HCASMCs in each image, and percentages of viable cells were calculated. Cellular droplets prior to printing were used for initial control for all groups.

3.9 Tissue histology

Histochemistry was applied to sections of vasculature. After 6 weeks of in vitro culturing in smooth muscle cell differentiation media, frozen vascular conduits were fixed and sectioned at 5 μm for histological examination for markers specific to smooth muscle cells. The Verhoeff–Van Giesen method was used to visualize elastic fiber formation and collagen deposition. Elastic fibers stain a blue black to black color, while collagen stains a red color. Samples were examined under an Olympus BX61 Brightfield Fluorescent microscope (Olympus America, Melville, NY, USA) at different magnifications.

3.10 Scanning electron microscopy (SEM) imaging

Immediately after fabrication, vascular conduits were soaked in a 4% CaCI2 solution for 12 hours to increase mechanical properties. In order to preparing vascular conduits samples for SEM images, the conduits were cut into short sections. Then, samples were dehydrated in graded ethanol solutions (from 25% to 100%). After the dehydration process, platinum used to coat the samples in order to increase image quality. These images were taken using a scanning electron microscope (Hitachi S-4800).

3.11 Statistical analysis

The statistical significance of experimental data for the mechanical and perfusion tests was determined by one way analysis of variance (ANOVA) with a significance level of $p < 0:05$ in Minitab 16. The paired wise test was combined with the Tukey posthoc test at a significance level of $p < 0.05$ and used for the cell viability study in the Statistical Package for the Social Sciences (SPSS). Three samples were used for each experimental group ($n = 3$).

CHAPTER IV

RESULTS

4.1 Fabrication

In this study, vascular conduits were fabricated using MWCNT-reinforced alginate and plain alginate (Figure 4.1(a)). The printed vascular structures were obtained in the form of conduits with well-defined tubular wall and lumen (Figure 4.1 (b)). The average inner and outer diameters of the fabricated vascular conduits were 461 ± 68 m and 930 ± 43 m, respectively. Vascular conduits were fabricated at more than a meter long with successful perfusion capability, demonstrating their functionality. Conduits could be manufactured at any desired length and pattern through printing without producing any occlusion or rupture that resulted in a leak or burst. Successful perfusion through a meter-long vascular conduit was achieved as shown in Figure 4.1 (c).

In addition, they were highly permeable, which enabled diffusion of media in a radial direction similar to natural blood vessels. Moreover, they could be printed layer by layer, and a 3D printed structure with eight layers or more was achieved (data not shown here). A vascular conduit with controllable dimensions in the micro- and sub-millimeter-scales can be printed by altering the process parameters. For example, Figure 4.1 (b) shows the wall and lumen under light microscopy. The wall dimensions could be controlled by controlling the process parameters, instantaneously resulting in varying diameters across the length.

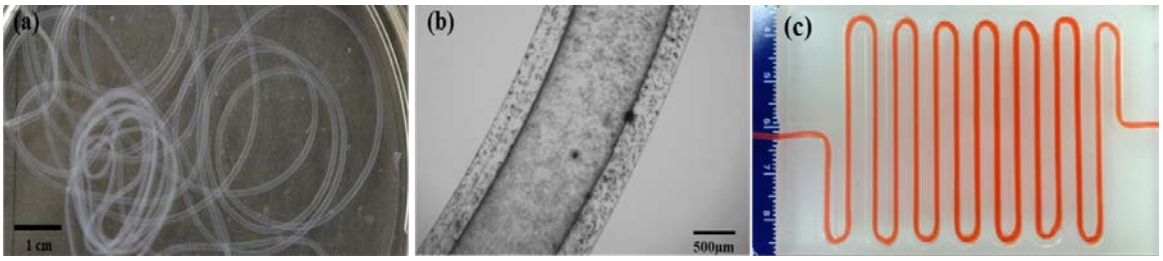

Figure 4.1

Sample vascular conduits: (a) printed vascular conduits, (b) a zoomed image under light microscopy showing the wall and lumen, and (c) cell media successfully perfused through a meter-long printed conduit.

4.2 Scanning electron microscopy (SEM) imaging

Scanning electron microscope (SEM) figures of vascular conduits with 1% MWCNT and plain alginate are shown in Figure 4.2. Figure 4.2 (a) shows the lumen of vascular conduits, where an acceptable cylindricity was obtained, demonstrating the morphological integrity of the conduits. Figure 4.2(b) shows the structure of a MWCNT-reinforced composite vascular conduit at the fracture, where fibrous MWCNTs are highlighted within the dashed rectangle. A similar structure did not appear in a 4% plain alginate conduit, as presented in Figure 4.2 (c). In both cases, sponge-like shapes were obtained at the fracture. The inner and outer walls of the vascular conduit are illustrated in Figures 4.2 (d) and (e), respectively. Deformation was observed to some extent during the dehydration process.

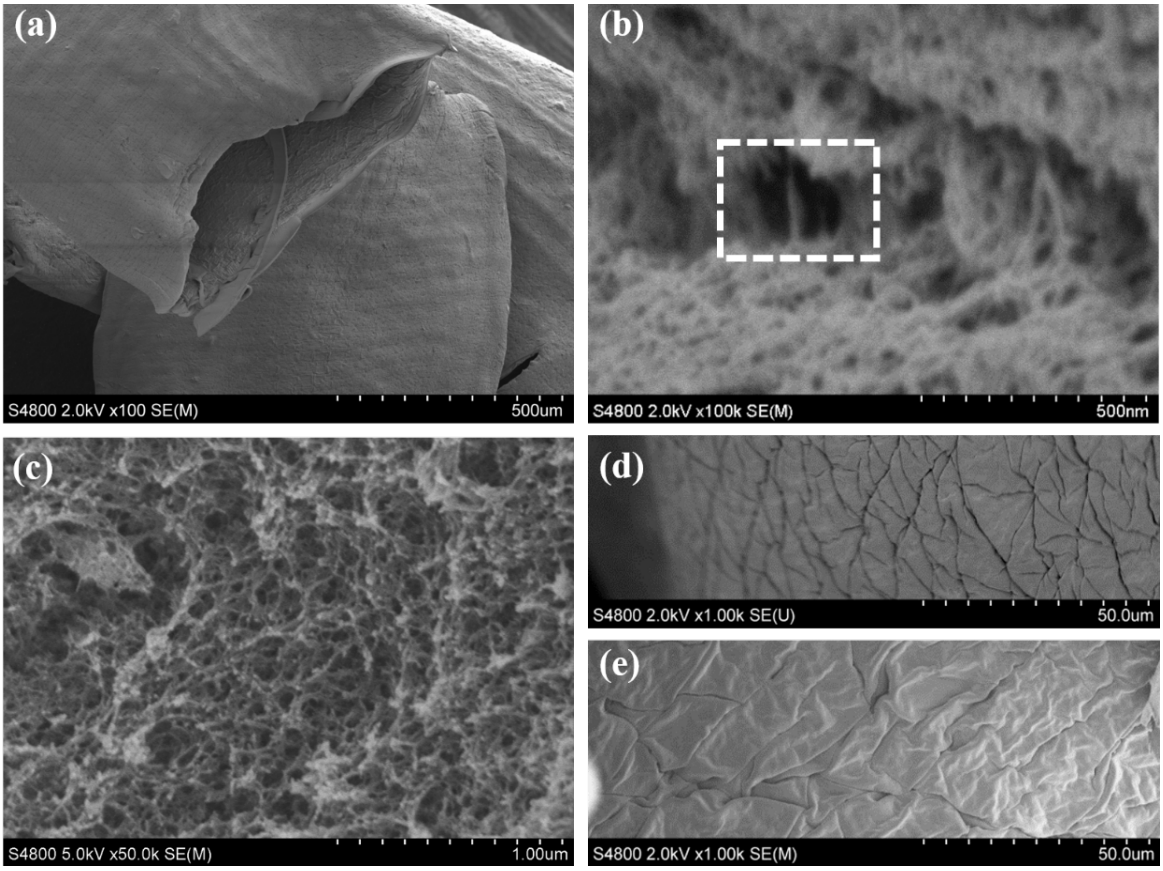

Figure 4.2

SEM images of vascular conduits: (a) structural integrity showing tubular shape, (b) 4% alginate reinforced with 1% MWCNTs with highlighted fibrous MWCNT at the fracture site of vascular conduits (see the dashed rectangle), (c) 4% plane alginate vasculature at the fracture site without appearance of fibrous shape in the spongy architecture, (d) inner wall of vascular conduit reinforced with 1% MWCNT, and (e) outer wall of vascular conduit reinforced with 1% MWCNT.

4.3 Mechanical characterization of vascular conduits

4.3.1 Tensile test

4.3.1.1 Tensile strength

The results of the tensile stress test showing tensile strength, elastic modulus and ultimate strain of vascular conduits for all types of samples are presented in Figures 4.3, 4.4, 4.5. From the plots, one can compare the mechanical properties of samples with and without MWCNT and different concentrations of biomaterial solution. Figure 4.3 (a) shows that the tensile strength increased significantly with each addition of MWCNT from 110 ± 5.8 kPa in 3% alginate only gels to 161 ± 24 kPa in gels with 0.5% MWCNT and 238 ± 14 kPa in gels with 1% MWCNT. The tensile strength of 4% alginate also increased with the inclusion of MWCNT from 382 ± 19 kPa in alginate alone gels to 420 ± 22 kPa in gels 0.5% MWCNT to 422 ± 22 kPa in gels with 1% MWCNT (Figure 4.3 (b)).

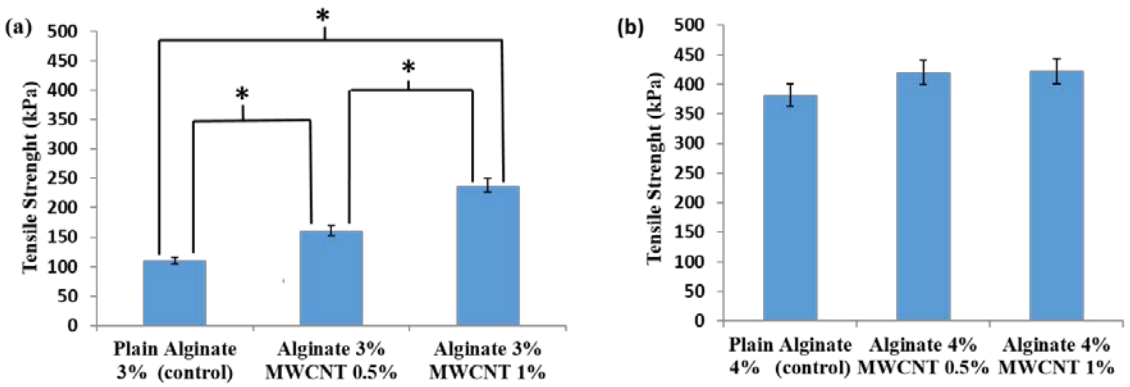

Figure 4.3

Comparison of tensile strength of: (a) 3% alginate with 0.5% and 1% MWCNT reinforced 3% alginate, (b) 4% plain alginate with 0.5% and 1% MWCNT-reinforced 4% alginate (* represents statistically significant difference $p < 0.05$).

4.3.1.2 Elastic modulus

As presented in Figure 4.4 (a), elastic modulus for 3% alginate gels also increased significantly with the addition of MWCNT, from 105 ± 7.5 kPa to 174 ± 13 kPa and 305 ± 17.5 kPa for alginate alone, alginate with 0.5% MWCNT and alginate with 1.0% MWCNT, respectively. Using the same reinforcement percentages, elastic modulus also increased from 341 ± 23 kPa to 593 ± 28 kPa and 667 ± 35 kPa for 4% alginate (Figure 4.4 (b)).

For groups in Figures 4.4 (a) and (b), there was a significant difference in the elastic modulus between plain alginate and the reinforced ones; however, no significant difference was observed in the elastic modulus between the reinforced ones with different MWCNT concentrations for 4%.

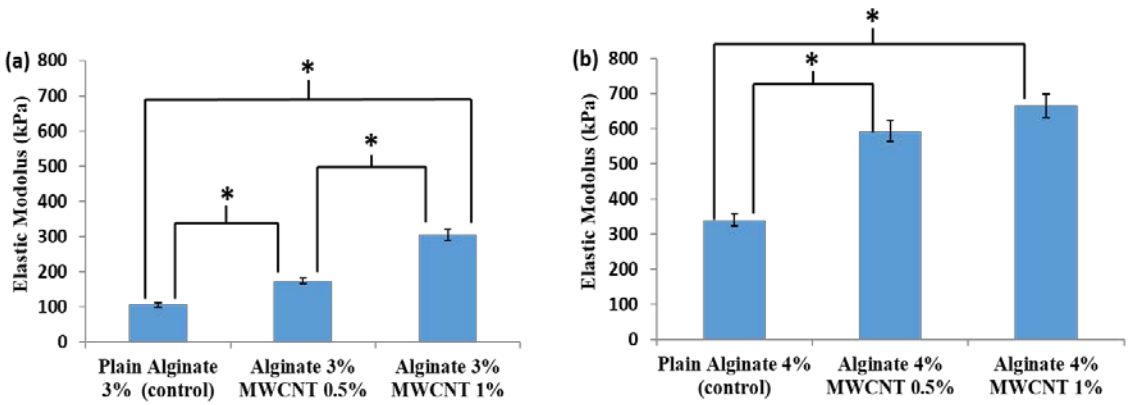

Figure 4.4

Comparison of elastic modulus of: (a) 3% plain alginate with 0.5% and 1% MWCNT-reinforced 3% alginate, (b) 4% plain alginate with 0.5% and 1% MWCNT-reinforced 4% alginate (* represents statistically significant difference $p < 0.05$).

4.3.1.3 Ultimate strain

In contrast to tensile strength and elastic modulus, ultimate strain decreased (though not significantly) for both 3% and 4% alginate gels as MWCNT concentration was increased (see Figures 4.5 (a) and (b)). In 3% alginate gels, ultimate strain decreased from 0.82 ± 0.18 to 0.79 ± 0.03 and 0.68 ± 0.18 for gel alone, gel with 0.5% MWCNT and gel with 1% MWCNT, respectively. In 4% alginate gels, ultimate strain decreased from 0.69 ± 0.09 to 0.68 ± 0.13 and 0.64 ± 0.22 for gel alone, gel with 0.5% MWCNT and gel with 1% MWCNT, respectively.

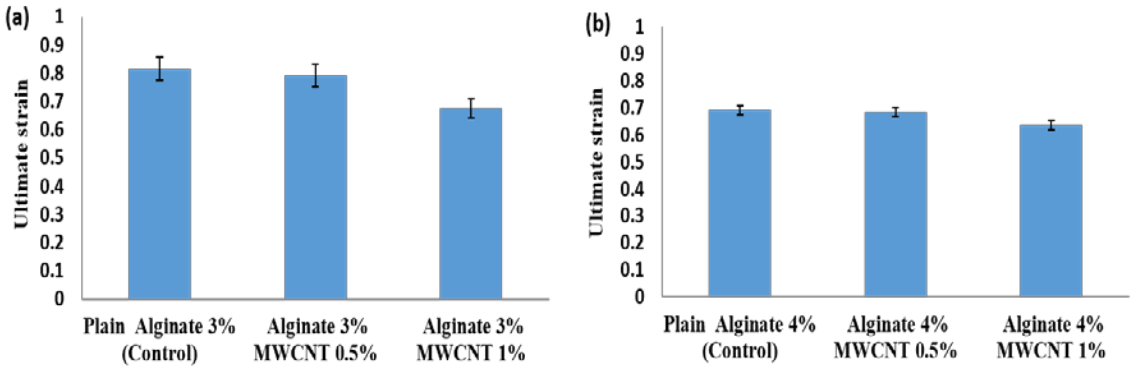

Figure 4.5

Comparison of ultimate strain of: (a) 3% plain alginate with 0.5% and 1% MWCNT-reinforced 3% alginate, (b) 4% plain alginate with 0.5% and 1% MWCNT-reinforced 4% (* represents statistically significant difference $p < 0.05$).

Samples with higher concentrations of alginate and MWCNT had higher tensile strength and elastic modulus and lower ultimate strain compared to samples with lower concentrations of these components. Differences in these mechanical properties can be explained in part by the properties of the alginate itself. The higher the concentration and viscosity of the alginate solution, the stronger the intermolecular interactions between polymer chains are and the more entanglements form [42]. Therefore, one would expect that the 4% alginate gel's increased tensile strength and elastic modulus and decreased ultimate strain can be attributed to greater cohesion between the polymer chains due to more physical entanglements. These could be due to distribution, dispersion and alignment of the MWCNT in alginate, which could affect the physical and mechanical properties and the orientation of nanomaterial along the vascular conduits. The addition of reinforcing MWCNT also affected the mechanical properties, although much more so in 3% alginate

gels than in 4% alginate gels. The distribution and dispersion of the MWCNT in alginate appears to affect the microstructure of the gel, which in turn can control the physical properties of the vascular conduits. The incorporation of MWCNT in a lower alginate solution likely improved the mechanical properties of the conduits more substantially than in the higher concentration alginate solutions due to the presence of fewer polymer chain entanglements. If the ratio of MWCNT to alginate concentration had been maintained for both 3% and 4% alginate gels, it is possible that the inclusion of MWCNT would have produced a stronger effect in the 4% gels.

4.4 Burst pressure

Based on Equation 5, the estimated burst pressure values are plotted in Figure 4.6. The estimated burst pressure of the vascular conduit for the control group, 0.5% MWCNT-reinforced group and 1% MWCNT-reinforced group were 208.14 mmHg, 215.89 mmHg and 221.65 mmHg, respectively. The 0.5% and 1% MWCNT reinforcement increased burst pressure by 3.7% and 6.5%.

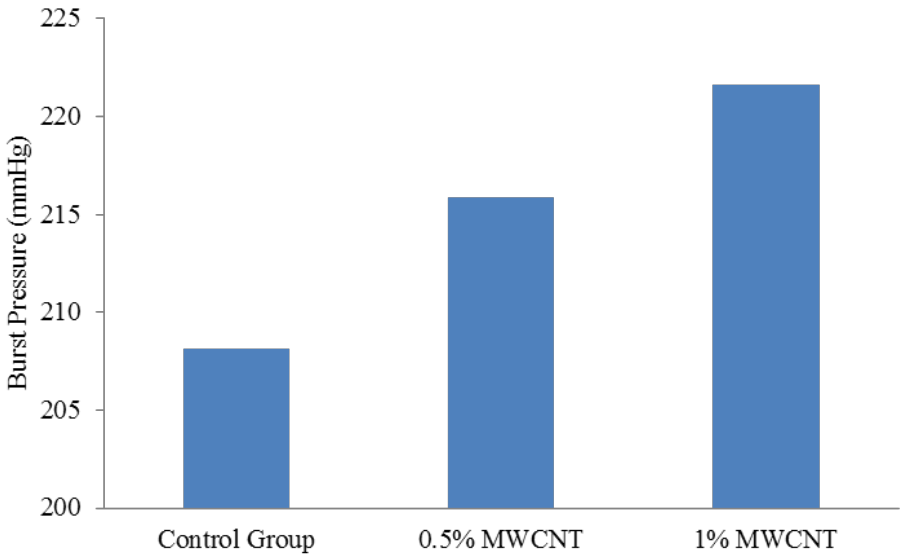

Figure 4.6

Comparison of burst pressure of 4% plain alginate with 0.5% and 1% MWCNT-reinforced vascular conduits with control group 4% plain alginate

4.5 Perfusion test

The results of the perfusion study show that all vascular conduits elongated from 8 to 8.4 ± 0.05 cm after one hour of media perfusion. This was primarily caused by the weight of vascular conduits. Due to gravity, the weight of the perfused media as well as the weight of the vascular conduit itself stretched the conduit toward the bottom of the perfusion chamber. Elongation terminated as long as the vascular conduit reached the bottom of the perfusion chamber. The diffusion rates for 3 h of perfusion are shown in Figure 4.7. The diffusion rate for 4% plain alginate, 4% plain alginate 0.5% MWCNT, and 4% alginate 1% MWCNT were 7.2 ± 0.48 µl min $^{-1}$, 8:4 ± 0.68 µl min $^{-1}$, and 7 ±0.71 µl min $^{-1}$,

respectively. No statistical difference was observed among those three groups, which might be due to the negligible effect of MWCNT reinforcement on the alginate polymer structure.

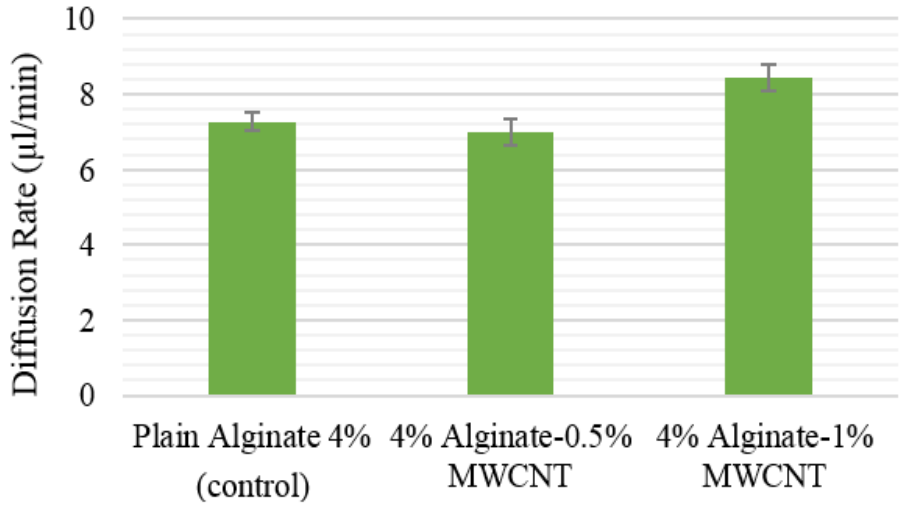

Figure 4.7

Effect of MWCNT concentration on diffusion rate of vascular conduits.

Although the 4% alginate to 1% MWCNT group had the highest diffusion rate, no statistical difference was observed among those three groups, which might be due to the negligible effect of MWCNT reinforcement on the permeability of the alginate polymer structure. In other words, the pore size of alginate polymer, which is approximately 30-450 nm for 4% [77], is much greater than the diameter of MWCNT (approximately 30 nm, according to the manufacturer's specifications), and hence the diffusion of media was not affected by the reinforcement of MWCNTs at low concentration. However, one can

speculate that the diffusion rate could decrease if the reinforcement concentration increased significantly.

4.6 Dehydration study

The experiments were conducted for an alginate vascular conduit after dehydration in order to find out the dimensional characterization (Figure 4.8). Only alginate vascular conduit diameter was measured since the wall thickness and lumen section were not visible under microscope. No statistical significant difference was observed between groups.

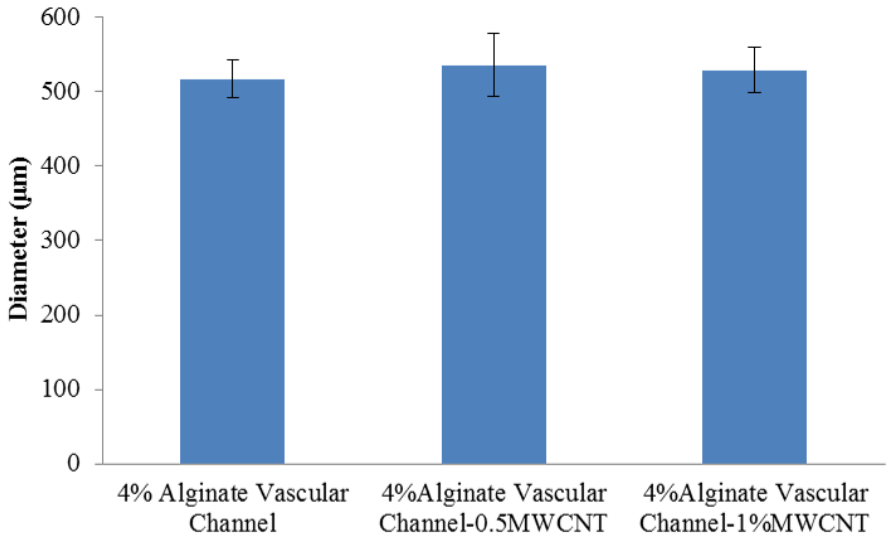

Figure 4.8

MWCNT reinforcing influence on alginate vascular conduits after dehydration

Figure 4.9 shows the alginate vascular conduits shrinkage by weight. There is an obvious difference between the groups that have an alginate vascular conduits with MWCNT reinforcing and the groups that have an alginate vascular conduits without MWCNT reinforcing, whereas the shrinkage rates of 1% MWCNT reinforcing and 0.5% MWCNT reinforcing are at similar levels, 61.48% and 62.30%, respectively. The three-dimensional vasculature shrinkage rate for 4% (w/v) alginate vascular conduit 4% (w/v) alginate vascular conduit with 0.5% MWCNT reinforcing, and 4% (w/v) alginate vascular conduit with 1% MWCNT reinforcing are 95.94%, 94.28% and 94.64%, respectively.

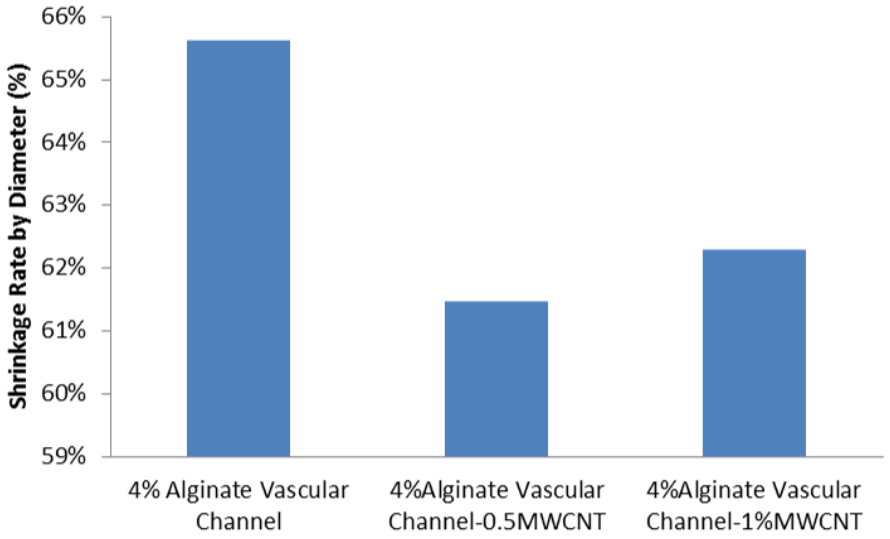

Figure 4.9

MWCNT reinforcing influence on shrinkage rate by diameter of alginate vascular conduit dehydration process

These numbers are similar and consistent with values of alginate vascular conduit shrinkage by weight (Figure 4.10). In measurements of alginate vascular conduit shrinkage by weight, the results of the 4% (w/v) alginate vascular conduit, 4% (w/v) alginate vascular conduit with 0.5% MWCNT reinforcing, and 4% (w/v) alginate vascular conduit with 1% MWCNT reinforcing are 94.64 ± 0.5%, 92.94 ± 0.06% and 92.54 ± 0.2%, respectively. There are significant differences between the groups that have an alginate vascular conduit with MWCNT reinforcing and those that have an alginate vascular conduit without MWCNT reinforcing. However, the difference between different MWCNT concentration groups is not significant.

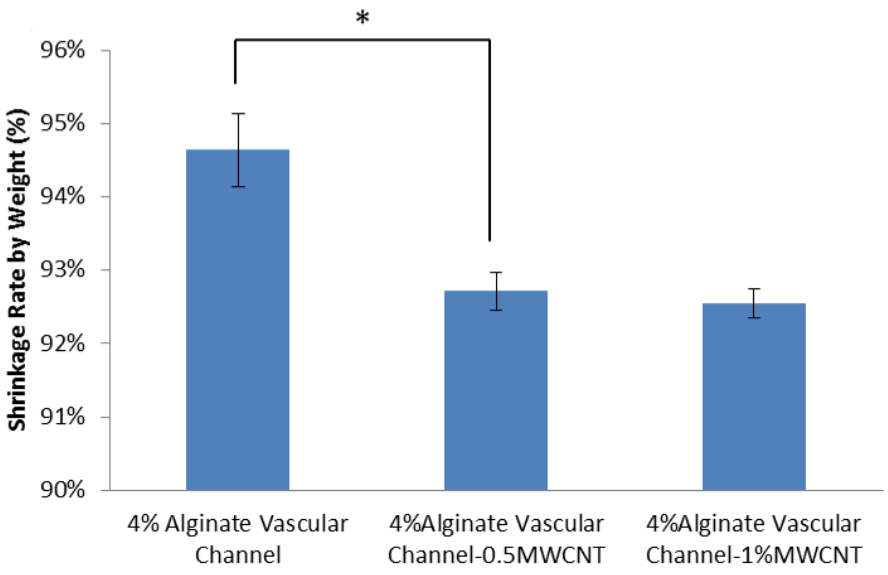

Figure 4.10

MWCNT reinforcing influence on shrinkage rate by weight of alginate vascular conduit dehydration process (* represents statistically significant difference $p < 0.05$).

4.7 Swelling and degradation studies

These studies were conducted to show how MWCNTs influence the alginate vascular conduit swelling and degradation properties. Figure 4.11 presents the swelling ratio graph for the 3% and 4% alginate reinforced with 0.5% and 1% MWCNT.

Figure 4.11 (a) illustrates that the sample with lower concentration of alginate and lower concentration of MWCNT (3% alginate reinforced with 0.5% MWCNT) has a higher swelling ratio than the other three samples that have higher concentrations of alginate and MWCNTs. As shown in Figure 4.11 (a), there was no significant difference between the four groups; this was due to the low concentrations of MWCNT in each sample. The average maximum swelling ratios for the 3% alginate reinforced with 0.5 % and 1% MWCNT and the 4% alginate reinforced with 0.5% and 1% MWCNT were 85%, 80%, 76% and 73%, respectively (Figure 4.11 (b)). W_i/W_o represents the vascular conduit liquid reabsorption capability where W_i is the instant sample weight at the measurement moments and W_o is the original sample weight. W_i/W_o for the sample of 3% alginate reinforced with 0.5% and 1% MWCNT and the 4% alginate reinforced with 0.5% and 1% MWCNT were 6.51%, 5.98%, 5.36% and 4.26%, respectively (Figure 4.11 (c)).

The amount of absorbent water was decreased by increasing the amount of MWCNT in the hydrogel of vascular conduits since the MWCNT group was not hydrophilic. The MWCNTs were irregularly distributed in the polymer network and prevent the penetration of water molecules into the network. Furthermore, since MWCNT was one of the agents of generating the vascular conduit's polymer network, it affects the absorption of the water. Hence, the samples with more MWCNT had the least liquid

absorption capability. On the other hand, increasing the concentration of the alginate decreases the water absorption capability because of the polymer chain entanglement. The higher the polymer concentration was, the higher the polymer chain entanglement and the lower the capability of liquid absorption.

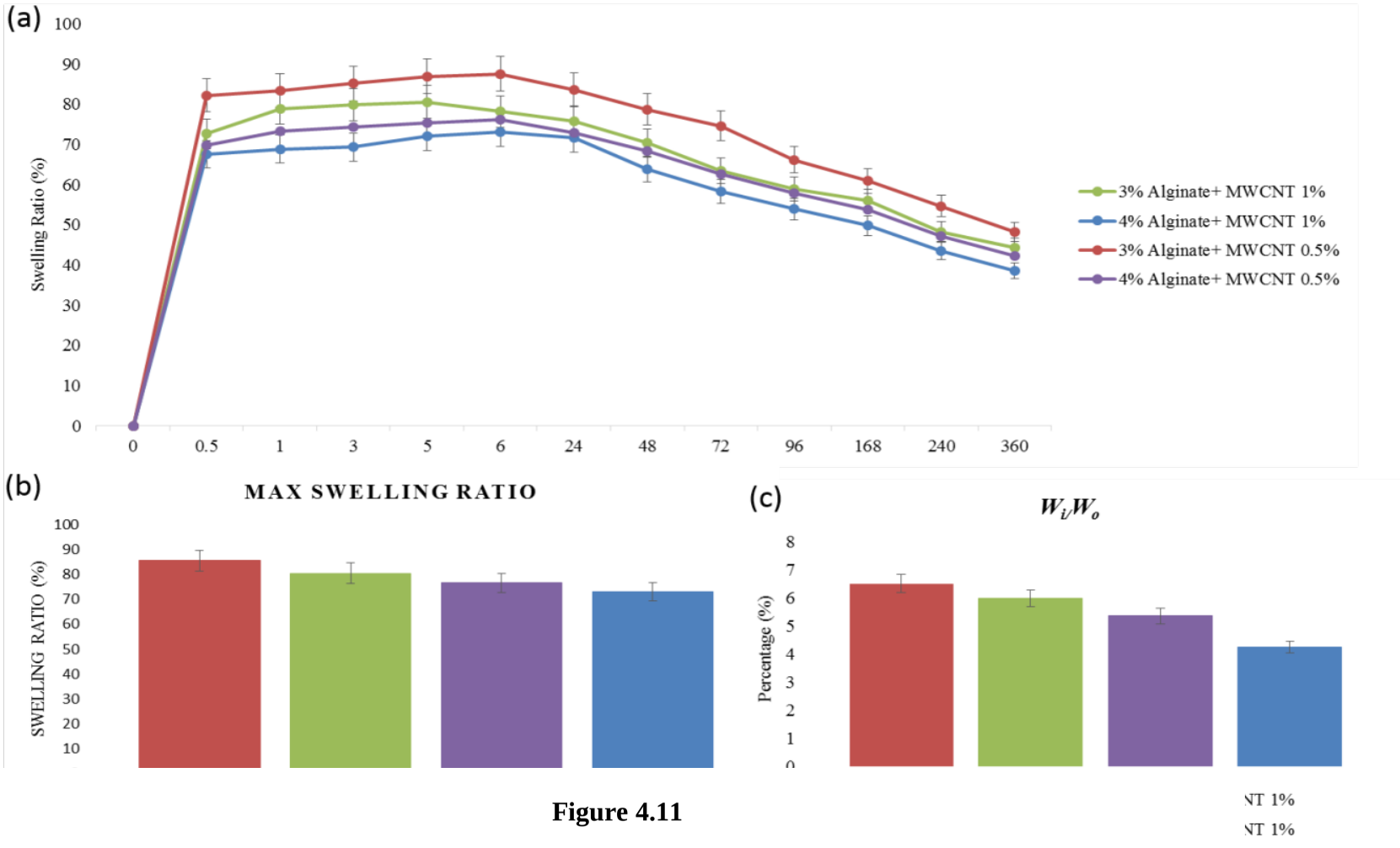

Figure 4.11

Influence of MWCNT reinforcement on vascular conduit in swelling process: (a) swelling ratio graph; (b) maximum swelling ratio and (c) vascular conduit liquid reabsorption capability.

4.8 Cell viability

As demonstrated in Figure 8(a), the printing process caused some cell damage; quantitative red fluorescent labeled dead cells were observed from the fluorescence image along the conduit channel wall. Compared with the initial control, cell viability was decreased from 75.6 ± 0.04% to 53.3 ± 0.01% for plain alginate vascular conduits, and from 72.2 ± 0.02% to 53.9 ± 0.01% for MWCNT reinforced upon printing (Figure 4.12).

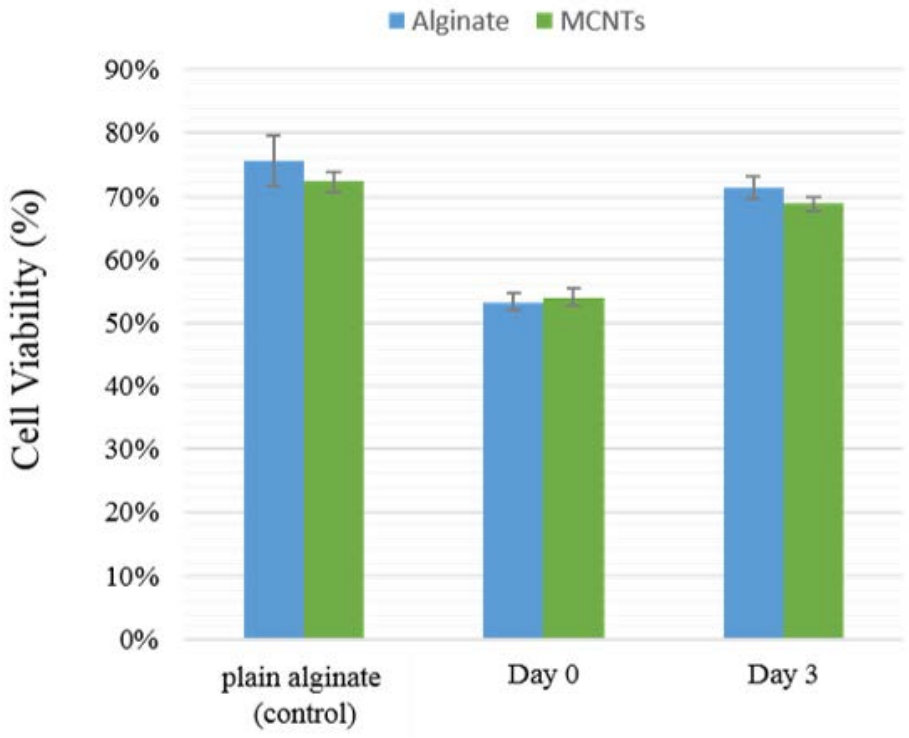

Figure 4.12

Cell viability over time in plain alginate vascular conduits and MWCNT reinforced ones.

Nevertheless, cells were able to recover from damage during in vitro culture after the printing process, as cell viability in day 3 reached 71.3 ± 0.02% and 68.8 ± 0.01% for plain alginate and MWCNT reinforced vascular conduits, respectively. These percentages were close to the initial control group. This demonstrated that cells were not completely dead, as shown in Figure 4.13; instead, they might be damaged to some extent and able to recover and grow in culture.

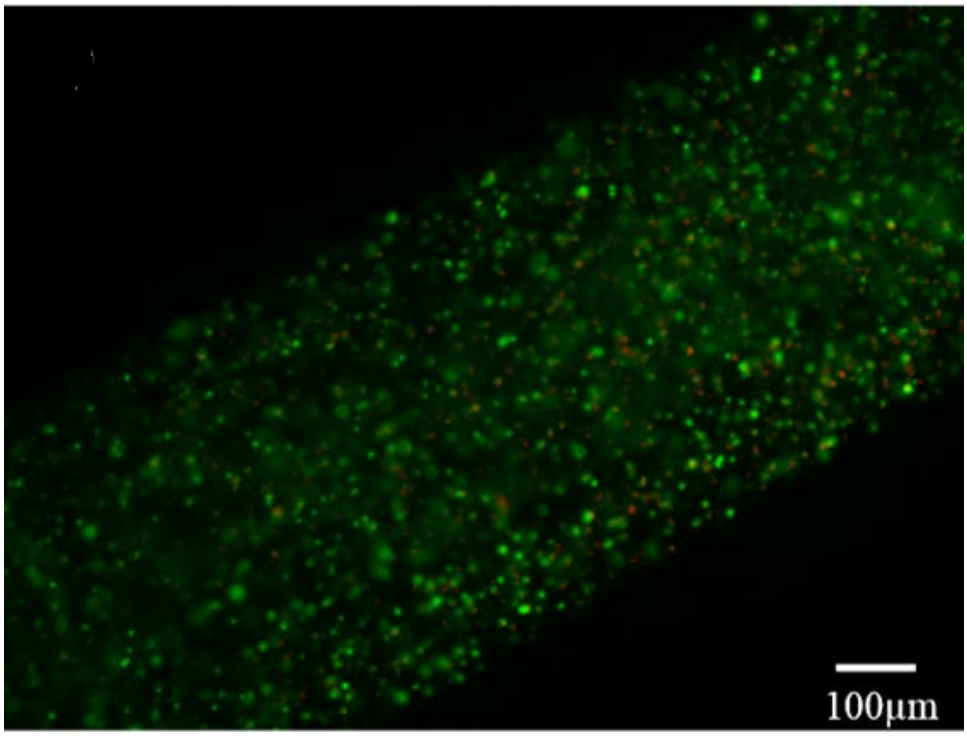

Figure 4.13

Fluorescent microscopic image from three-day-cultured MWCNT-reinforced vascular conduit showed most of the cells are viable (green); a minimal amount of dead cells (red) were also observed.

No significant difference was observed between the control group and the MWCNT reinforced ones. Thus, the low concentration of MWCNT reinforcement in this research did not affect the viability of HCASMC in short-term in vitro culture; however, biodegradable nanofibers are preferred for long-term culture or in vivo studies because the living environment cannot absorb CNTs by natural means.

4.9 Tissue histology

The long-term biocompatibility of vascular conduits with MWCNT reinforcement was evaluated through histochemistry study by checking cell morphology and tissue-specific ECM formation. The tissue histology study showed different characteristics between MWCNT-free (the positive control group) and MWCNT-reinforced conduits. In MWCNT-reinforced conduits, damaged cells within the conduit wall can be easily identified by broken cell nuclei, as indicated by the red arrowheads in Figures 4.14 (a) and (b).

In CNT-free conduits, the majority of the cells were intact, with rounded nuclei uniformly distributed within the conduit wall (Figure 4.14 (c), blue arrowheads). Some live cells were still observed, as shown in Figure 4.14 (b). In addition, a number of cells migrated to the outermost section of the conduit wall and proliferated, forming a well-aligned cellular layer with substantial ECM formation, as shown in the dashed box in Figure 4.14 (c) In MWCNT-reinforced conduits, almost no ECM formation was observed, which might be due to the toxicity effect of MWCNTs in the long run that restricted cells from performing their biological functions properly. The failure of ECM formation might have resulted from MWCNT altering the cellular function or viability, which could result in a cytotoxic result.

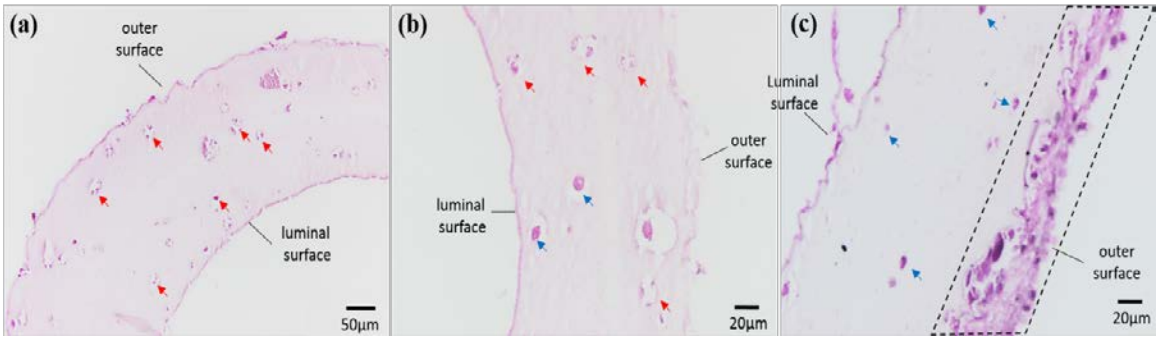

Figure 4.14

Histochemistry of CNT-reinforced conduits: (a) transverse section showing damaged cells (shown with red arrows) within disintegrated nuclei in the MWCNT-reinforced conduit, (b) radial longitudinal section showing damaged cells (shown with red arrows) within the MWCNT-reinforced conduit wall, (c) positive control group without CNT reinforcement, where cells were healthy (shown with blue arrows) and produced substantial matrix in the outer section of the wall in 6 weeks (highlighted in the dashed box).

In addition, the dashed box in Figure 4.14 (c) also shows that, in MWCNT-reinforced conduits, elastin and collagen were stained negative. On the other hand, plain conduits stained positive for collagen, as shown in Figure 4.14 (c) and stained positive for elastin in some other histological sections.

CHAPTER V

DISCUSSIONS

Our experiments with printing CNT-reinforced vascular conduits successfully demonstrated the use of sodium alginate because of its appealing gelation properties, which are highly suitable for the coaxial printing process. Using printing, complex shapes in 3D can be fabricated through layer-by-layer stacking of vascular conduits. In general, vascular conduits with an external diameter ranging from 500 µm to 2 mm and a lumen diameter ranging from 150 µm to 1 mm can be printed using the demonstrated system. One of the major advantages of the introduced bioprinting process is that it enables direct printing of the vascular conduits without the need for any temporary support material that is to be removed thereafter, such as thermo-sensitive hydrogels, i.e., agarose and collagen.

In order to fabricate functional vascular conduits, one should ensure that the mechanical, structural, biological and perfusion capabilities of vascular conduits are acceptable. In our experiments, we reached an 8.2 ± 0:3 µl min $^{-1}$ diffusion rate within three hours of perfusion, which enabled high viability of encapsulated cells due to the super-diffusive properties of alginate. As alginate concentration increases, mesh network size diminishes, and a compact structure forms, resulting in slower diffusion of the media [78]. In the meantime, mechanical and structural characteristics of the vascular conduits decrease as the material concentration increases.

In general, viability and cell migration capability decrease as the concentration of alginate increases. Thus, there is a tradeoff between functionality and the cell viability and

biological performance of the conduits. Our initial trials with low concentrations of alginate, such as 2.5%, showed that the bioprinting system did not produce structurally well-defined, mechanically acceptable perfusable conduits. Most of the time, the vascular conduits collapsed when low concentration ranges were used. Therefore, nanofiber reinforcement (such as natural polymers and proteins) might be ideal for enhancing the mechanical, structural and perfusion characteristics of vascular conduits with biologically reasonable properties.

Carbon nanotube reinforcement increased the ultimate tensile stress by 11% and the modulus of elasticity by 94%. It decreased the ultimate strain by 18%. We achieved 70% cell viability three days post-printing, which increased thereafter in short-term culture. In general, cells proliferate and reach over 90% viability in a week [62]. Particularly, the reinforcement enhanced the mechanical properties of low-concentration alginate. The improvement of ultimate tensile stress and elastic modulus demonstrated that the stress was transferred between the hydrogel matrix and the CNTs reinforcing the vascular conduit's composites. In addition, the external stress was effectively transferred from the alginate matrix to the reinforced MWCNTs through the better bonded interfaces in alginate-reinforced MWCNT composites [79, 80]. The interfacial adhesion between CNTs and the matrix is one of the crucial factors affecting the mechanical properties of the composites. In fact, MWCNTs have a greater affinity to the polymer matrix, resulting in a significant improvement in mechanical properties [79, 80].

As demonstrated in the histology images, cells within CNT-reinforced conduits were damaged and underwent cell death. They were not able to repopulate or to produce ECM in the long term. Nevertheless, in plain vascular conduits (the positive control group),

cells were largely intact and were able to migrate and proliferate towards the outer section of the channel wall. We can speculate that it was probably guided by the media gradient during culture, since the outer section interacted with cell culture media extensively, especially smooth muscle cell growth factors. Also, repopulated cells were able to produce intercellular ECM and form a sheet covering the outer section of the channel wall. Some matrix formation was observed in the inner surface of the wall as a lining, and that was separated from the wall during the cutting process of the histology study. However, matrix formation in the inner surface could be improved by keeping the pulsatile media flow through the lumen. In this way, HCASMCs could align their proliferation with respect to the pulsatile flow as in the natural blood vessels. Although a cell viability test showed acceptable cell viability in CNT-reinforced conduits in short-term culture, only a limited number of cells were able to survive and carry out their functions properly in long-term culture.

CHAPTER VI

CONCLUSION AND FUTURE DIRECTIONS

In this study, we demonstrated a new practical technique for vasculature fabrication, where micro-vascular conduits were directly printed using a coaxial nozzle configuration. Vascular conduits in this thesis were reinforced with CNTs to improve the mechanical properties that are essential for further applications such as generating blood vessels or producing supplement vasculatures for engineered tissues. Mechanical and perfusion testing was conducted for CNT-reinforced vascular conduits, and biological characterization was performed in the short and long term to understand cellular viability and ECM formation. Although short-term results were acceptable, CNT-induced toxicity reduced the biological performance of the conduits. In terms of biocompatibility, MWCNT reinforcement did not significantly affect cell viability in the short term compared with plain conduits, but it did impede cell survival as well as motility and ability to synthesize ECM in the long term. Optimization to achieve reasonable biocompatibility could be expected in future studies.

In sum, this thesis provides a foundation for direct printing of mechanically reinforced vascular conduits, where CNTs could be replaced with natural polymer nanofibers for further applications such as scale-up tissue fabrication or blood vessel generation. The effectiveness of natural polymer fibers has already been demonstrated in the literature [81]. For future studies, reinforce electrospun collagen type I nanofibers along with lower percentages of polymer solution could be applied and generate an endothelial lining inside the lumen to biomimetically fabricate a vasculature network. It will promote

oxygenation and media transport, be a part of the hybrid tissue in a short period of time, and eventually degrade.

Electro-spinning is an ideal process for generating continuous nano-fibers with the desired diameter, fiber deposition and orientation of fibers in a mesh with a variety of natural and synthetic polymers by applying high-voltage power to the tip of spinneret nozzle and controlling the deposition of fibers on a grounded collector [82, 83]. Several natural and synthetic polymers have been used extensively in this process in order to fabricate continuous nano-fibers in the range of nanometers to micrometers [66, 82, 83]. An electro-spinning setup apparatus, shown in Figure 6.1, consists of a high-voltage power supply, a nozzle or spinneret, a syringe pump and a ground collector plate.

By applying electrical high-voltage power on the external surface of the metal nozzle of the spinneret, an electrical field is generated between the nozzle with positive polarity and the ground collector with the negative polarity. In this process, when the electrical field reaches its critical range, it overcomes the surface tension force of the polymer solution and forms an electrically charged jet. The range of the electrical field will be different for each material due to its conductivity and concentration. In addition, a polymer solution will be prepared by completely dissolving the polymer material in an appropriate solvent. During the jetting of the polymer from the needle tip to the collector, the solvent is evaporated and, finally, nano-fibers are deposited on the ground collector.

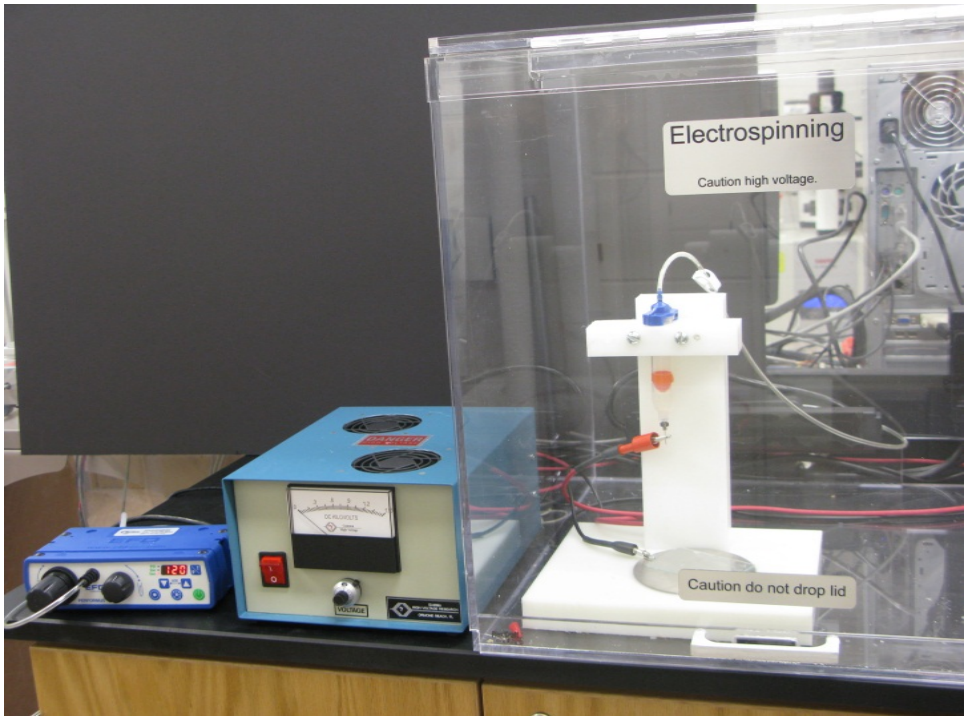

Figure 6.1

An electro-spinning setup

The main advantages of electro-spinning are the fact that it is a rapid, efficient and inexpensive technique [82, 84]. Furthermore, the variety of application fields and its versatility have made this process very interesting to researchers. One of the significant applications of electrsospun nano-fibers is in tissue engineering, wound dressing and drug delivery[82, 85]. Its widespread applications, ability to generate complex and three-dimensional scaffolds, and the potential of the desired structural, functional and biological properties of electrospun nano-fibers have made electro-spinning an interesting technique for researchers over the past few decades [82, 84, 85].

Since collagen is the most abundant protein family (30%) in the human body and the principal structural element of extra-cellular matrix (ECM), collagen fibers will mimic the structural and biological properties of natural collagen [84]. This chapter highlights electro-spinning techniques, fabrication of collagen nano-fibers, the application of collagen fibers and the parameters affected in this process. In addition, fabrication of tissue engineering scaffolds with collagen nano-fibers is investigated.

This chapter demonstrated that it is possible to proportionate high mechanical strength into a matrix by controlling nano-fiber orientation and thickness. The electrospun collagen scaffold is an ideal remedy for those who have suffered the loss of an organ. Despite their benefit in improving the mechanical properties of conduits, CNTs have side effects such as toxicity in long-term culture or in vivo testing [86]. Thus, in order to exploit the mechanical benefits of printed fiber composites, other nontoxic materials should be investigated. Biodegradable materials, such as polylactide, polyglycolide, and its derivatives, can be added to alginate in the form of nanofibers to increase the mechanical strength of conduits while also increasing biocompatibility for cell growth and function [87]. Alternatively, short extruded collagen fibers that exist on the mm micron scale could be added for a similar effect [81]. Collagen type I and elastin are the essential components of natural blood vessels that give ultimate mechanical properties (strength and elasticity). Matrix deposition including these proteins was observed in the positive control group, and reinforcing them further during the printing process could improve the mechanobiological characteristics of the vascular conduits considerably. In this regard, the fabricated vascular conduits can be tested in vivo safely for long-term monitoring of the performance of the conduits. In addition, other biodegradable materials such as polylactide and its derivatives

can be added to alginate in the form of nanofibers to increase the mechanical strength of conduits while also increasing biocompatibility for cell growth and function.

REFERENCES

1. *Donate the gift of life*. 2013, U.S. Department of Health and Human Service.
2. Böttcher-Haberzeth, S., Thomas Biedermann, and Ernst Reichmann, *Tissue engineering of skin.* Burns, 2010. **36**(4): p. 450-460.
3. Ma, L., Changyou Gao, Zhengwei Mao, Jie Zhou, Jiacong Shen, Xueqing Hu, and Chunmao Han, *Collagen/chitosan porous scaffolds with improved biostability for skin tissue engineering.* Biomaterials, 2003. **24**(6): p. 4833-4841.
4. Mei, L., Deyu Hu, Jianfeng Ma, Xiping Wang, Yunzhi Yang, and Jinsong Liu, *Preparation, characterization and evaluation of chitosan macroporous for potential application in skin tissue engineering.* International journal of biological macromolecules, 2012. **51**(5): p. 992-997.
5. Paquet, C., Danielle Larouche, Francis Bisson, Stéphanie Proulx, Carolyne Simard-Bisson, Manon Gaudreault, Hubert Robitaille et al., *Tissue engineering of skin and cornea.* Annals of the New York Academy of Sciences, 2010. **1197**(1): p. 166-177.
6. Mondy, W.L., Don Cameron, Jean-Pierre Timmermans, Nora De Clerck, Alexander Sasov, Christophe Casteleyn, and Les A. Piegl, *Computer-aided design of microvasculature systems for use in vascular scaffold production.* Biofabrication, 2009. **1**(3): p. 035002.
7. Naito, Y., Toshiharu Shinoka, Daniel Duncan, Narutoshi Hibino, Daniel Solomon, Muriel Cleary, Animesh Rathore, Corey Fein, Spencer Church, and Christopher Breuer, *Vascular tissue engineering: Towards the next generation vascular grafts.* Advanced drug delivery reviews, 2011. **63**(4): p. 312-323.
8. Norotte, C., Francois S. Marga, Laura E. Niklason, and Gabor Forgacs, *Scaffold-free vascular tissue engineering using bioprinting.* Biomaterials, 2009. **30**(30): p. 5910-5917.
9. Schmidt, C.E., and Jennie M. Baier, *Acellular vascular tissues: natural biomaterials for tissue repair and tissue engineering.* Biomaterials, 2000. **21**(22): p. 2215-2231.
10. Skardal, A., Jianxing Zhang, and Glenn D. Prestwich, *Bioprinting vessel-like constructs using hyaluronan hydrogels crosslinked with tetrahedral polyethylene glycol tetracrylates.* Biomaterials, 2010. **31**(24): p. 6173-6181.
11. Zhao, L., Vivian K. Lee, Seung-Schik Yoo, Guohao Dai, and Xavier Intes, *The integration of 3-D cell printing and mesoscopic fluorescence molecular tomography of vascular constructs within thick hydrogel scaffolds.* Biomaterials, 2012. **33**(21): p. 5325-5332.
12. Holzwarth, J.M., and Peter X. Ma., *Biomimetic nanofibrous scaffolds for bone tissue engineering.* Biomaterials, 2011. **32**(36): p. 9622-9629.
13. Tian, H., Shantaram Bharadwaj, Yan Liu, Haiyun Ma, Peter X. Ma, Anthony Atala, and Yuanyuan Zhang, *Myogenic differentiation of human bone marrow mesenchymal stem cells on a 3D nano fibrous scaffold for bladder tissue engineering.* Biomaterials, 2010. **31**(5): p. 870-877.
14. Chen, T., Matthew J. Hilton, Edward B. Brown, Michael J. Zuscik, and Hani A. Awad, *Engineering superficial zone features in tissue engineered cartilage.* Biotechnology and bioengineering, 2013. **110**(5): p. 1476-1486.

15. Sanchez-Adams, J., and Kyriacos A. Athanasiou, *Athanasiou, Dermis isolated adult stem cells for cartilage tissue engineering.* Biomaterials, 2012. **33**(1): p. 109-119.
16. Chen, A.A., David K. Thomas, Luvena L. Ong, Robert E. Schwartz, Todd R. Golub, and Sangeeta N. Bhatia, *Humanized mice with ectopic artificial liver tissues.* Proceedings of the National Academy of Sciences, 2011. **108**(29): p. 11842-11847.
17. Lee, J.S., and Seung-Woo Cho. , *Liver tissue engineering: Recent advances in the development of a bio-artificial liver.* Biotechnology and Bioprocess Engineering, 2012. **17**(3): p. 427-438.
18. Shinoka, T., Christpher K. Breuer, Ronn E. Tanel, Gregor Zund, Takuya Miura, Peter X. Ma, Robert Langer, Joseph P. Vacanti, and John E. Mayer Jr, *Tissue engineering heart valves: Valve leaflet replacement study in a lamb model.* The Annals of thoracic surgery, 1995. **60**: p. S513-S516.
19. Bader, A., Tobias Schilling, Omke Enno Teebken, Gudrun Brandes, Tanja Herden, Gustav Steinhoff, and Axel Haverich, *Tissue engineering of heart valves–human endothelial cell seeding of detergent acellularized porcine valves.* European journal of cardio-thoracic surgery, 1998. **14**(3): p. 279-284.
20. Sebinger, D.D., Andreas Ofenbauer, Petra Gruber, Susann Malik, and Carsten Werner, *ECM modulated early kidney development in embryonic organ culture.* biomaterials, 2013. **34**(28): p. 6670-6682.
21. Cieslinski, D.A., and H. David Humes, *Tissue engineering of a bioartificial kidney*. Biotechnology and bioengineering, 1994. **43**(7): p. 678-681.
22. Choi, N.W., Mario Cabodi, Brittany Held, Jason P. Gleghorn, Lawrence J. Bonassar, and Abraham D. Stroock. , *Microfluidic scaffolds for tissue engineering.* Nature materials, 2007. **6**(11): p. 908-915.
23. Yow, K.-H., J. Ingram, S. A. Korossis, E. Ingham, and S. Homer-Vanniasinkam, *Tissue engineering of vascular conduits* Br. J. Surg. , 2006. **93**: p. 652–61.
24. Lee, W., Vivian Lee, Samuel Polio, Phillip Keegan, Jong-Hwan Lee, Krisztina Fischer, Je-Kyun Park, and Seung-Schik Yoo., *On-demand three-dimensional freeform fabrication of multi-layered hydrogel scaffold with fluidic channels.* Biotechnology and bioengineering, 2010. **105**(6): p. 1178-1186.
25. Nemeno-Guanzon, J.G., Soojung Lee, Johan Robert Berg, Yong Hwa Jo, Jee Eun Yeo, Bo Mi Nam, Yong-Gon Koh, and Jeong Ik Lee, *Trends in tissue engineering for blood vessels.* BioMed Research International, 2012.
26. Dee, K.C., David A. Puleo, and Rena Bizios, *An introduction to tissue biomaterial interactions.* John Wiley & Sons, 2003.
27. Intranuovo, F., Roberto Gristina, Francesco Brun, Sara Mohammadi, Giacomo Ceccone, Eloisa Sardella, François Rossi, Giuliana Tromba, and Pietro Favia. , *Plasma Modification of PCL Porous Scaffolds Fabricated by Solvent-Casting/Particulate-Leaching for Tissue Engineering.* Plasma Processes and Polymers, 2014. **11**(2): p. 184-195.
28. Sin, D., Xigeng Miao, Gang Liu, Fan Wei, Gary Chadwick, Cheng Yan, and Thor Friis, *Polyurethane (PU) scaffolds prepared by solvent casting/particulate leaching (SCPL) combined with centrifugation.* Materials Science and Engineering: C, 2010. **30**(1): p. 78-85.

29. Edwards, S.L., W. Mitchell, J. B. Matthews, E. Ingham, and S. J. Russell, *Design of nonwoven scaffold structures for tissue engineering of the anterior cruciate ligament.* Autex Res J, 2004. **4**(2): p. 86-94.
30. Nazarov, R., Hyoung-Joon Jin, and David L. Kaplan, *Porous 3-D scaffolds from regenerated silk fibroin.* Biomacromolecules, 2004. **5**(3): p. 718-726.
31. Haugh, M.G., Ciara M. Murphy, and Fergal J. O'Brien, *Novel freeze-drying methods to produce a range of collagen–glycosaminoglycan scaffolds with tailored mean pore sizes.* Tissue Engineering Part C: Methods, 2009. **16**(5): p. 887-894.
32. O'Brien, F.J., Brendan A. Harley, Ioannis V. Yannas, and Lorna Gibson, *Influence of freezing rate on pore structure in freeze-dried collagen-GAG scaffolds.* Biomaterials, 2004. **25**(6): p. 1077-1086.
33. Yoshimoto, H., Y. M. Shin, H. Terai, and J. P. Vacanti, *A biodegradable nanofiber scaffold by electrospinning and its potential for bone tissue engineering.* Biomaterials, 2003. **24**(12): p. 2077-2082.
34. Ozbolat, I.T., and Yin Yu, *Bioprinting toward organ fabrication: challenges and future trends.* IEEE transactions on bio-medical engineering, 2013. **60**(3): p. 691-699.
35. Cho, S.-W., Sang Hyun Lim, Il-Kwon Kim, Yoo Sun Hong, Sang-Soo Kim, Kyung Jong Yoo, Hyun-Young Park et al, *Small-Diameter Blood Vessels Engineered With Bone Marrow–Derived Cells.* Annals of surgery, 2005. **241**(3): p. 506.
36. Kaushal, S., Gilad E. Amiel, Kristine J. Guleserian, Oz M. Shapira, Tjorvi Perry, Fraser W. Sutherland, Elena Rabkin et al. , *Functional small-diameter neovessels created using endothelial progenitor cells expanded ex vivo.* Nature medicine, 2001. **7**(9): p. 1035-1040.
37. L'Heureux, N., Nathalie Dusserre, Gerhardt Konig, Braden Victor, Paul Keire, Thomas N. Wight, Nicolas AF Chronos et al., *Human tissue engineered blood vessels for adult arterial revascularization.* Nature Med, 2006. **12**: p. 361–5.
38. Caves, J.M., Vivek A. Kumar, Adam W. Martinez, Jeong Kim, Carrie M. Ripberger, Carolyn A. Haller, and Elliot L. Chaikof., *The use of microfiber composites of elastin-like protein matrix reinforced with synthetic collagen in the design of vascular grafts.* Biomaterials, 2010. **31**(27): p. 7175-7182.
39. Watanabe, M., Toshiharu Shin'oka, Satoshi Tohyama, Narutoshi Hibino, Takeshi Konuma, Gohki Matsumura, Yoshimichi Kosaka et al., *Tissue-engineered vascular autograft: inferior vena cava replacement in a dog model.* Tissue engineering 2001. **7**(4): p. 429-439.
40. Ozawa, F., Kosuke Ino, Yasufumi Takahashi, Hitoshi Shiku, and Tomokazu Matsue, *Electrodeposition of alginate gels for construction of vascular-like structures* Journal of bioscience and bioengineering, 2013. **115**(4): p. 459-461.
41. Stegemann, J.P., and Robert M. Nerem, *Phenotype modulation in vascular tissue engineering using biochemical and mechanical stimulation.* Annals of biomedical engineering, 2003. **31**(4): p. 391-402.
42. Khalil, S. *Deposition and Structure Formation of 3 D Alginate Tissue Engineering*. [PhD Dissertation] 2006.
43. Dahl, S.L., Jennifer Koh, Vikas Prabhakar, and Laura E. Niklason. , *Decellularized native and engineered arterial scaffolds for transplantation.* Cell transplantation, 2003. **12**(6): p. 659-666.

44. Sheridan, W.S., Garry P. Duffy, and B. P. Murphy. , *Mechanical characterization of a customized decellularized scaffold for vascular tissue engineering.* Journal of the Mechanical Behavior of Biomedical Materials, 2012. **8**: p. 58-70.
45. Gilbert, T.W., Tiffany L. Sellaro, and Stephen F. Badylak, *Decellularization of tissues and organs.* Biomaterials, 2006. **27**(19): p. 3675-3683.
46. Isenberg, B.C., Yukiko Tsuda, Corin Williams, Tatsuya Shimizu, Masayuki Yamato, Teruo Okano, and Joyce Y. Wong., *A thermoresponsive, microtextured substrate for cell sheet engineering with defined structural organization.* Biomaterials, 2008. **29**(17): p. 2565-2572.
47. McClendon, M.T., and Samuel I. Stupp, *Tubular hydrogels of circumferentially aligned nanofibers to encapsulate and orient vascular cells.* Biomaterials, 2012. **33**(23): p. 5713-5722.
48. Mironov, V., Vladimir Kasyanov, Christopher Drake, and Roger R. Markwald, *Organ printing: promises and challenges.* 2008.
49. Yildirim, E., X. Yin, S. Guceri, and W. Sun, *A preliminary study on using multi nozzle polymer deposition system to fabricate composite alginate/carbon nanotube tissue scaffolds.* Solid Freeform Fabrication Symp: p. 84-95.
50. Kai, D., Molamma P. Prabhakaran, Benjamin Stahl, Markus Eblenkamp, Erich Wintermantel, and Seeram Ramakrishna., *Mechanical properties and in vitro behavior of nanofiber–hydrogel composites for tissue engineering applications.* Nanotechnology 2012. **23**: p. 095705.
51. Shin, H., Seongbong Jo, and Antonios G. Mikos, *Biomimetic materials for tissue engineering.* Biomaterials, 2003. **24**(24): p. 4353-4364.
52. Ma, P.X., *Biomimetic materials for tissue engineering.* Advanced drug delivery reviews, 2008. **60**(2): p. 184-198.
53. Patterson, J., Mikaël M. Martino, and Jeffrey A. Hubbell, *Biomimetic materials in tissue engineering.* Materials today, 2010. **13**(1): p. 14-22.
54. Dee, K.C., David A. Puleo, and Rena Bizios., *An introduction to tissue-biomaterial interactions.* 2003.
55. Guelcher, S.A., and Jeffrey O. Hollinger, eds., *An introduction to biomaterials*. 2006: CRC/Taylor & Francis.
56. Coleman, J.N., Umar Khan, Werner J. Blau, and Yurii K. Gun'ko., *Small but strong: a review of the mechanical properties of carbon nanotube.* polymer composites Carbon 2006. **44**: p. 1624-1652.
57. Bu H, K.A.L., Knudsen K D and Nystr¨om B *Rheological and structural properties of aqueous alginate during gelation via the Ugi multicomponent condensation reaction.* Biomacromolecules 2004. **5**: p. 1470-9.
58. Augst, A.D., Hyun Joon Kong, and David J. Mooney, *Alginate hydrogels as biomaterials Macromol.* 6, 2006: p. 623-633.
59. Zhang, Y., Yin Yu, Farzaneh Dolati, and Ibrahim T. Ozbolat., *Effect of multiwall carbon nanotube reinforcement on coaxially extruded cellular vascular conduits.* Materials Science and Engineering: C, 2014. **39**(0): p. 126-133.
60. Spitalsky, Z., Dimitrios Tasis, Konstantinos Papagelis, and Costas Galiotis, *Carbon nanotube–polymer composites: chemistry, processing, mechanical and electrical properties Prog.* Polym. Sci. , 2010. **35**: p. 357-401

61. Yakobson, B.I., and Phaedon Avouris, *Mechanical properties of carbon nanotubes* Carbon nanotubes. Springer Berlin Heidelberg, 2001: p. 287–327.
62. Zhang, Y., Yin Yu, Howard Chen, and Ibrahim T. Ozbolat, *Characterization of printable cellular microfluidic channels for tissue engineering.* Biofabrication, 2013. **5**: p. 5004.
63. Hoerstrup, S.P., Alexander Kadner, Christian Breymann, Christine F. Maurus, Christina I. Guenter, Ralf Sodian, Jeroen F. Visjager, Gregor Zund, and Marko I. Turina, *Living, autologous pulmonary artery conduits tissue engineered from human umbilical cord cells.* The Annals of thoracic surgery, 2002. **74**(1): p. 46-52.
64. Ling, Y., Jamie Rubin, Yuting Deng, Catherine Huang, Utkan Demirci, Jeffrey M. Karp, and Ali Khademhosseini, *A cell-laden microfluidic hydrogel.* Lab on a Chip, 2007. **7**(6): p. 756-762.
65. Salvetat, J.-P., J-M. Bonard, N. H. Thomson, A. J. Kulik, L. Forro, W. Benoit, and L. Zuppiroli, *Mechanical properties of carbon nanotubes* Applied Physics A, 1999. **69**: p. 255-60.
66. Yang, L., Carel FC Fitie, Kees O. van der Werf, Martin L. Bennink, Pieter J. Dijkstra, and Jan Feijen, *Mechanical properties of single electrospun collagen type I fibers.* Biomaterials, 2008. **29**(8): p. 955-962.
67. Gauvin, R., Maxime Guillemette, Todd Galbraith, Jean-Michel Bourget, Danielle Larouche, Hugo Marcoux, David Aubé, Cindy Hayward, François A. Auger, and Lucie Germain, *Mechanical properties of tissue-engineered vascular constructs produced using arterial or venous cells.* Tissue Engineering Part A, 2011. **17**(15-16): p. 2049-2059.
68. Yildirim, E.D., Xi Yin, Kalyani Nair, and Wei Sun, *Fabrication, characterization, and biocompatibility of single-walled carbon nanotube-reinforced alginate composite scaffolds manufactured using freeform fabrication technique* J. Biomed. Mater. Res. B 2008. **87**: p. 406-414.
69. Andrews, R., and M. C. Weisenberger, *Carbon nanotube polymer composites* Current Opinion in Solid State and Materials Science, 2004. **8**: p. 31-37.
70. Lobo, A.O., E. F. Antunes, A. H. A. Machado, C. Pacheco-Soares, V. J. Trava-Airoldi, and E. J. Corat, *Cell viability and adhesion on as grown multiwall carbon nanotube films.* Material Science and Engineering, 2008. **28**: p. 264-9.
71. Mazzatenta, A., Michele Giugliano, Stephane Campidelli, Luca Gambazzi, Luca Businaro, Henry Markram, Maurizio Prato, and Laura Ballerini, *Interfacing neurons with carbon nanotubes: electrical signal transfer and synaptic stimulation in cultured brain circuits.* . The Journal of neuroscience, 2007. **27**(26): p. 6931-6936.
72. Hu, H., Yingchun Ni, Vedrana Montana, Robert C. Haddon, and Vladimir Parpura., *Chemically functionalized carbon nanotubes as substrates for neuronal growth.* Nano Lett, 2004. **4**: p. 507-11.
73. Mattson, M.P., Robert C. Haddon, and Apparao M. Rao, *Molecular functionalization of carbon nanotubes and use as substrates for neuronal growth.* Nano Lett, 2000. **4**: p. 507-11.
74. Verdejo, R., Gavin Jell, Laleh Safinia, Alexander Bismarck, Molly M. Stevens, and Milo SP Shaffer, *Reactive polyurethane carbon nanotube foams and their*

interactions with osteoblasts. ournal of Biomedical Materials Research Part A, 2009. **88**(1): p. 65-73.

75. Hoerstrup, S.P., Gregor Zünd, Ralf Sodian, Andrea M. Schnell, Jürg Grünenfelder, and Marko I. Turina, *Tissue engineering of small caliber vascular grafts.* European journal of cardio-thoracic surgery, 2001. **20**(1): p. 164-169.
76. Smith, B., Kevin Wepasnick, Kaitlin E. Schrote, Hyun-Hee Cho, William P. Ball, and D. Howard Fairbrother, *Influence of surface oxides on the colloidal stability of multiwalled carbon nanotubes: a structure–property relationship* Langmuir, 2009. **25**: p. 9767-76.
77. Chan, A.W., and Ronald J. Neufeld, *Modeling the controllable pH-responsive swelling and pore size of networked alginate based biomaterials.* Biomaterials, 2009. **30**(30): p. 6119-6129.
78. Ozbolat, I.T., and Bahattin Koc, *3D hybrid wound devices for spatiotemporally controlled release kinetics.* Comput. Methods Programs Biomed, 2012. **108**: p. 922-931.
79. Thostenson, E.T., and Tsu-Wei Chou, *Aligned multi walled carbon nanotube reinforced composites: processing and mechanical characterization* J. Phys. D: Appl. Phys, 2002. **35**.
80. Boccaccini, A.R., and Lutz Christian Gerhardt, *Carbon nanotube composite scaffolds and coatings for tissue engineering applications.* Key Engineering Materials, 2010. **441**: p. 31-52.
81. Gentleman, E., E. A. Nauman, K. C. Dee, and G. A. Livesay, *Short collagen fibers provide control of contraction and permeability in fibro blast seeded collagen gels* Tissue Engineering, 2004. **10**(3-4): p. 421-7.
82. Bhardwaj, N., and Subhas C. Kundu, *Electrospinning: a fascinating fiber fabrication technique.* Biotechnology advances, 2010. **28**(3): p. 325-347.
83. Fang, J., HaiTao Niu, Tong Lin, and XunGai Wang, *Applications of electrospun nanofibers.* Chinese Science Bulletin, 2008. **53**(15): p. 2265-2286.
84. Matthews, J.A., Gary E. Wnek, David G. Simpson, and Gary L. Bowlin, *Electrospinning of collagen nanofibers.* Biomacromolecules, 2002. **3**(2): p. 232-238.
85. Li, D., and Younan Xia., *Electrospinning of nanofibers: reinventing the wheel?* Advanced materials, 2004. **16**(14): p. 1151-1170.
86. Magrez, A., Sandor Kasas, Valérie Salicio, Nathalie Pasquier, Jin Won Seo, Marco Celio, Stefan Catsicas, Beat Schwaller, and László Forró, *Cellular toxicity of carbon based nanomaterials.* Nano Lett. , 2006. **6**: p. 1121-5.
87. Rim, N.G., Choongsoo S. Shin, and Heungsoo Shin, *Current approaches to electrospun nanofibers for tissue engineering* Biomed. Mater. , 2013. **8**: p. 4102.